ANALYSIS OF A POISSON-DRIVEN STOCHASTIC COVID-19 AND HEPATITIS B CO-INFECTION MODEL

Michael A. Pobbi[1], Samuel M. Naandam [2], and Stephen E. Moore[3]

[1]Department of Mathematics, University of Cape Coast, Ghana.
[2]Department of Mathematics, University of Cape Coast, Ghana.
[3]Department of Mathematics, University of Cape Coast, Ghana.

August 7, 2025

Abstract

In this article, we formulate and analyse a mathematical model for the co-infection of Hepatitis B virus and COVID-19. We incorporate into our framework Hepatitis B virus prevention, COVID-19 prevention, COVID-19 vaccination, and environmental factors so as to investigate their effect on transmission dynamics. First, we derive the basic reproduction number for HBV only, COVID-19 only, and co-infection stochastic models using the next generation matrix method. Next, we establish the conditions for stability in the stochastic sense for HBV only, COVID-19 only sub-models, and the co-infection model. Furthermore, we devote our attention to finding sufficient conditions for extinction and persistence. Finally, by using the Euler–Murayama scheme, we illustrate the dynamics of the co-infection, COVID-19, HBV and the effect of some parameters on disease transmission dynamics by means of numerical simulations.

Keywords: COVID-19, Hepatitis, Stochastic model, Lévy noise, Global Stability, Extinction.

1 Introduction

Hepatitis B disease is a life-threatening and infectious disease caused by the hepatitis B virus and is associated with serious liver infection, leading to liver malfunction, including cirrhosis, liver fibrosis, and hepatocellular carcinoma. The virus is typically transmitted from mother to child during birth and delivery, in early childhood, as well as through contact with blood, semen, or other body fluids from an infected person [61]. Between 8 weeks and 5 months, the exposed individual can experience symptoms including fever, loss of appetite, joint pain, fatigue, and nausea [12].

It remains a global health challenge, despite the development of antiviral therapies and the success of immunization [18]. Currently over 81 million people, from WHO African Region are chronically infected[3]. It is estimated that about 2 billion people are infected with HBV globally, with about 1.5 million infections annually [30], and 0.6 million annual deaths from HBV-related liver diseases [31, 6]. Countries such as Ghana, continue to have much higher (from 8.36% to

12.3%) disease prevalence rate than the global average of 3% [61] and approximately 294 HBV-related deaths weekly [13].

COVID-19, on the other hand, is caused by Severe Acute Respiratory Syndrome Corona virus 2 (SARS-CoV-2) and affects the functionality of the respiratory system. It spreads from person to person via direct contact with respiratory droplets from an infected individual. It can also be spread by touching surfaces contaminated with the virus and then touching the face. Since its emergence from Wuhan, China in December, 2019, it rapidly spread to every country and has inflicted severe public health and socio-economic burden globally [23]. It is estimated that over 7 million COVID-19 deaths and over 700 million infections have been reported since December 2019 [48]. Vaccination efforts have aided in reducing severe illness, hospitalizations, and deaths [48] worldwide. After a fourth transmission wave, Ghana also experienced a decline in COVID-19 cases. However, in July 2025, 107 confirmed cases were reported, underscoring the potential for seasonal resurgence [47].

Both COVID-19 and Hepatitis B virus (HBV) infections are life-threatening diseases and remain health problems particularly in Sub-Saharan African countries like Ghana, Botswana, and Nigeria, see, e.g., [48, 61]. Some clinical studies have confirmed the possibility of the co-infection of COVID-19 and Hepatitis B diseases, see, e.g., [63, 66, 58]. To improve understanding of the co-infection dynamics of these two global threats, mathematical models have been developed to address gaps in clinical studies and propose potential control strategies, see, e.g. [65, 56, 3, 1, 59]. In [56], the author, constructed and analysed a deterministic mathematical model that captures the co-infection dynamics of hepatitis B virus (HBV) and COVID-19 and also evaluated the impact of various intervention strategies, on the spread of both diseases in a population. In another study [59], a deterministic model was used to analyse the impact of optimal control strategies on the transmission of COVID-19 and HBV co-infection. [3] applied the Atangana-Baleanu fractional-order derivative to study a co-infection model for HBV and COVID-19. Meanwhile, [1] incorporated Gaussian noise to model the perturbations affecting the dynamics of COVID-19 and HBV co-infection. Although such studies have made significant contributions to understanding the dynamics of COVID-19 and HBV co-infection, they did not include COVID-19 vaccination, COVID-19 prevention, HBV prevention, and the combined effects of standard random fluctuations and large-scale disturbances caused by environmental factors within the same framework. This gap in the literature motivated the present work.

Several deterministic models have been developed to study the transmission dynamics of other infectious disease e.g. [15, 32, 52, 55, 29]. Stochastic models, however, provide a more nuanced understanding of disease spread, e.g., [10, 15, 41]. These epidemiological models, unlike classical deterministic counterparts, e.g. [19, 42, 54], account for the effects of random fluctuations in disease transmission dynamics, recovery rates, and the potential for co-infection by multiple diseases. To help explain the long run behaviour of disease spread, other studies such as [69, 38, 51] have presented analyses of the existence, uniqueness, and persistence of solutions to their stochastic models. In this article, we also employ suitable Lyapunov functions to develop conditions for extinction and persistence for the proposed co-infection model.

Despite advances in immunization, both HBV and COVID-19 continue to pose significant public health challenges [18, 63]. Co-infection of HBV and COVID-19 can exacerbate disease severity, leading to adverse outcomes, including increased mortality risk [66, 58]. Predicting long-term trends in the prevalence of HBV and COVID-19 co-infection, as well as identifying effective control mechanisms, is therefore essential for informed public health decision-making.

Specifically, our study seeks to investigate the following objectives;

1. To develop a compartmental model for the transmission dynamics of HBV-COVID-19 co-infection.
2. To establish the Invariance and Positivity of the Lévy driven stochastic co-infection model.
3. To determine the basic Reproductive number for deterministic and Stochastic co-infection models respectively.
4. To determine conditions for stability at Disease Free Equilibrium for deterministic and Stochastic co-infection models.
5. To present numerical simulations of the model.

The rest of the paper is organized as follows; Section (2) discusses the Mathematical Model and the underlying assumptions. In Section (3) , we analyze the COVID-19, HBV sub-models as well as the co-infection model. Section (4) is devoted to discussing the numerical method and numerical simulation of the model. Finally, we present the conclusion in Section (5).

2 Mathematical Model Formulation

In this section, we consider a stochastic compartmental mathematical model that uses differential equations, see Figure (1).

2.1 Assumptions of the model

The following assumptions are used to formulate the model.

(A_1) It is assumed that recruitment into the susceptible populations is by birth and immigration.

(A_2) New human infection is through close contact with infectious humans, and contaminated environments.

(A_3) It is assumed that there is homogeneous mixing in both sub-populations.

(A_4) COVID-19 vaccination wears off after some period of time.

(A_5) The total human population $N(t)$ is a sum of all the different compartments, i.e.

$$\begin{aligned} N(t) = S(t) + I_C(t) + I_a(t) + I_{aC}(t) + I_c(t) + I_{cC}(t) + T_a(t) \\ + T_C(t) + T_{aC}(t) + R_a(t) + R_C(t) + R_{aC}(t) + V_C(t). \end{aligned} \tag{1}$$

(A_6) There is no relapse from HBV recovery to Susceptible state. HBV recovered recovered persons generally develop lifelong immunity and cannot be reinfected. There is, however, relapse from COVID-19 recovered state to susceptible state.

(A_7) We assume that individuals with chronic HBV will remain in chronic HBV state, even if some form of medical management is administered. However they can be infected by COVID-19.

(A_8) There is no vertical transmission of HBV.

2.2 Human Population

The model is structured into thirteen human compartments. The subpopulations of the human population at time t, denoted by $N(t)$, The sub-populations of the human population at time t, denoted by $N(t)$, include susceptible individuals $S(t)$,COVID-19 infected individuals $I_C(t)$, acute hepatitis-B infected individuals $I_a(t)$, acute hepatitis-B infected and COVID-19 individuals $I_{aC}(t)$, chronic hepatitis-B infected individuals $I_c(t)$, chronic hepatitis-B and COVID-19 infected individuals $I_{cC}(t)$, acute hepatitis-B infected individuals receiving treatment $T_a(t)$, COVID-19 infected individuals receiving treatment $T_C(t)$, acute hepatitis-B and COVID-19 co-infected individuals receiving treatment $T_{aC}(t)$, acute hepatitis-B recovered individuals $R_a(t)$, COVID-19 recovered infected individuals $R_C(t)$, acute hepatitis-B and COVID-19 recovered individuals $R_{aC}(t)$, and COVID-19 vaccinated individuals $V_C(t)$.

The model, as seen from Figure 1, excludes HBV vaccination compartment. This is because we consider a typically high HBV prevalence population with low HBV vaccinated population (i. e., Ghana data used in estimating infections rates are typically based on such unvaccinated population). Further, HBV vaccine provides long-lasting immunity which will imply such persons can only be infected by COVID-19.

2.3 Model Formulation

In this section, we consider a stochastic compartmental mathematical model that uses differential equations. Figure 1 presents the flow between states of the COVID-19 and HBV co-infection model.

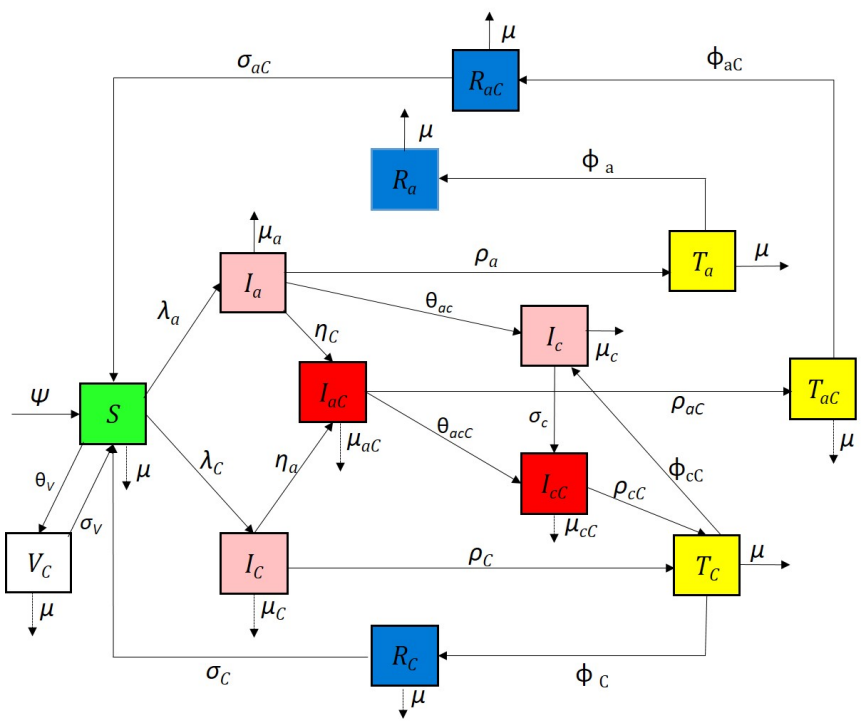

Figure 1: Compartmental diagram for the COVID-19 and Hepatitis B co-infection cohort.

We obtain the following system of non-linear differential equations from the model flow diagrams of the disease transmission shown in Figure 1.

$$
\begin{cases}
\dfrac{dS(t)}{dt} & = \psi + \sigma_V V_C(t) + \sigma_{aC} R_{aC}(t) + \sigma_C R_C(t) - (\lambda_a I_a(t) + \lambda_C I_C(t))S(t) \\
& \quad -(\mu + \theta_V)S(t) \\
\dfrac{dI_a(t)}{dt} & = \lambda_a I_a(t)S(t) - (\theta_{ac} + \rho_a + \eta_C I_{aC}(t) + \mu_a)I_a(t) \\
\dfrac{dI_C(t)}{dt} & = \lambda_C I_C(t)S(t) - (\eta_a I_{aC}(t) + \rho_C + \mu_C)I_C(t) \\
\dfrac{dI_{aC}(t)}{dt} & = (\eta_C I_a(t) + \eta_a I_C(t))I_{aC}(t) - (\rho_{aC} + \theta_{acC} + \mu_{aC})I_{aC}(t) \\
\dfrac{dI_c(t)}{dt} & = \theta_{ac} I_a(t) + \phi_{cC} T_C(t) - (\sigma_c + \mu_c)I_c(t) \\
\dfrac{dI_{cC}(t)}{dt} & = \sigma_c I_c(t) + \theta_{acC} I_{aC}(t) - (\mu_{cC} + \rho_{cC})I_{cC}(t) \\
\dfrac{dT_a(t)}{dt} & = \rho_a I_a(t) - (\mu + \phi_a)T_a(t) \\
\dfrac{dT_{aC}(t)}{dt} & = \rho_{aC} I_{aC}(t) - (\mu + \phi_{aC})T_{aC}(t) \\
\dfrac{dT_C(t)}{dt} & = \rho_{cC} I_{cC}(t) + \rho_C I_C(t) - (\mu + \phi_C + \phi_{cC})T_C(t) \\
\dfrac{dR_a(t)}{dt} & = \phi_a T_a(t) - \mu R_a(t) \\
\dfrac{dR_{aC}(t)}{dt} & = \phi_{aC} T_{aC}(t) - (\mu + \sigma_{aC})R_{aC}(t) \\
\dfrac{dR_C(t)}{dt} & = \phi_C T_C(t) - (\mu + \sigma_C)R_C(t) \\
\dfrac{dV_C(t)}{dt} & = \theta_V S(t) - (\mu + \sigma_V)V_C(t),
\end{cases}
\tag{2}
$$

with initial conditions $S(0) > 0$, $I_C(0) \geq 0$, $I_a(0) \geq 0$, $I_{aC}(0) \geq 0$, $I_c(0) \geq 0$, $I_{cC}(0) \geq 0$, $T_a(0) \geq 0$, $T_C(0) \geq 0$, $T_{aC}(0) \geq 0$, $R_a(0) \geq 0$, $R_C(0) \geq 0$, $R_{aC}(0) \geq 0$, $V_C(0) \geq 0$.

λ_C, λ_a are the transmission rate for COVID-19, and HBV respectively. The parameters ψ, λ_C, η_C, λ_a, θ_{aC}, θ_{acC}, ρ_a, ρ_{aC}, ρ_C, ϕ_{aC}, ϕ_a, ϕ_C, σ_V, σ_C, σ_{aC}, θ_V, μ, μ_C, μ_{aC}, μ_a, μ_c, and μ_{cC} are non-negative, with a forces of infection $\omega_C = \lambda_C I_C = \beta_C(1 - \kappa\zeta)I_C(t)/N$, and $\omega_a = \lambda_a I_a = \beta_a(1 - \delta\zeta)I_a(t)/N$ respectively, and $\eta_a = \omega_a$, and $\eta_C = \omega_C$. κ and δ are fraction of the community employing protective or preventive measures for COVID-19 and HBV respectively, and ζ is the efficacy of personal protection strategy adopted.

The model parameters along with their description are provided in Table 1.

Table 1: Parameters and description

Parameter	Description of Parameters
ψ	Recruitment rates of human
θ_{ac}	Progression rate from acute to chronic HBV state
β_C	COVID-19 spreading rate
β_a	HBV spreading rate
θ_{acC}	Progression rate of acute HBV co-infection to chronic HBV dual infection.
ρ_a	Treatment for acute HBV infected
ρ_{aC}	COVID-19 Treatment rate for acute HBV and COVID-19 infected individuals
ρ_C	Treatment for COVID-19 infected
ρ_{cC}	Treatment for COVID-19 infected in chronic HBV co-infected
ϕ_{aC}	Recovery rate for co-infected
ϕ_a	Recovery rate for acute HBV infected
ϕ_C,	Recovery rate for COVID-19 infected individuals
σ_V	COVID-19 Vaccinated immunity waning rate
σ_C	COVID-19 recovered immunity waning rate
σ_{aC}	COVID-19 recovered immunity waning rate for acute HBV co-infected
θ_V	COVID-19 vaccination rate
μ	Natural Death rate of humans
μ_C	Death rate IN COVID-19 Infected state
μ_{aC}	Death rate in Acute HBV and COVID-19 co-infected state
μ_a	Death rate in Acute HBV state
μ_c	Death rate in Chronic HBV state
μ_{cC}	Death rate in Chronic HBV and COVID-19 co-infected state
κ	Fraction of the community employing COVID protective measures
δ	Fraction of the community employing HBV preventive measures
ζ	Efficacy of personal protection strategy adopted

Two popular ways to introduce stochastic factors into epidemic models are: (i) to assume some small and standard random fluctuation, (ii) to assume massive disturbances caused by sudden environmental shocks. The first, is described by Brownian noise while the second is described by the Lévy-driven jumps.

In this study, it is assumed that fluctuations in the environment will manifest mainly as fluctuations in the parameter β, i.e. $\beta \longrightarrow \beta + \epsilon_i dB_i(t)$, $(i = 1, 2, ..., 13)$, where $dB_i(t)$ is a one dimensional standard Brownian noise with $B_i(0) = 0$, and ϵ_i is the intensity of the noise. Details on how this was done in the study is detailed as follows.

With regards to jumps, we restrict Lévy noise to COVID-19 infectious states. This involved the inclusion of a multiplicative jump noise which occurs randomly and proportional the number of infective in a finite population, e.g., [1]. Biological justification for the above stems from the fact that COVID-19 spreads through human interactions, and can be highly irregular due to spreader factors. Such factors, e.g., mass gatherings at funeral ceremonies and loose enforcement of public health measures (e.g., wearing of nose masks) are mentioned in Ghanaian studies, see, e.g., [46] as

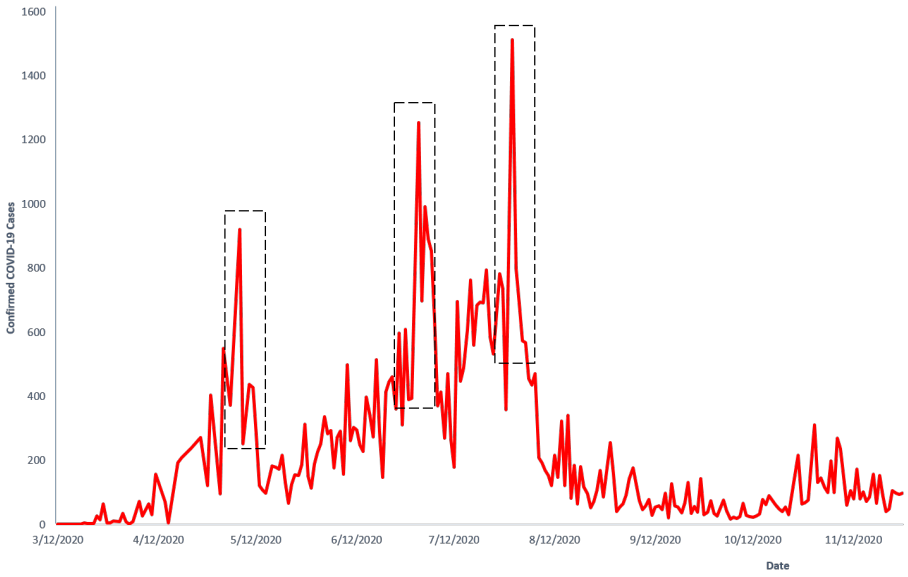

Figure 2: Confirmed COVID-19 cases in Ghana. [53]

causes of COVID-19 jumps in the distribution of disease spread. It is observed from Figure 2 that the distribution of confirmed COVID-19 data from Ghana exhibited jumps as a result of factors outlined by [46].

Jumps are excluded in HBV. Only Brownian noise is included in the HBV infectious states as disease spread in real world data for in population considered, see, e.g.,[22] do not exhibit the presence of jumps (i.e., infection rate remains relative smooth). Hence, $I(t)dB_I(t)$ accounts for continuous fluctuations in transmission.

The Poisson-driven Lévy process, thus, is divided into linear drift term, Brownian motion and finite Lévy driven noise. The stochastic model of the system (2) takes the following form:

$$
\begin{cases}
\dfrac{dS(t)}{dt} & = \psi + \sigma_V V_C(t) + \sigma_{aC} R_{aC}(t) + \sigma_C R_C(t) - (\lambda_a I_a(t) + \lambda_C I_C(t))S(t) \\
& \quad -(\mu + \theta_V)S(t) + \epsilon_1 S(t) dB_1(t) + \int_{\mathcal{U}} \Psi_1(u) S(s^-) \tilde{\mathcal{N}}(dt, du) \\
\dfrac{dI_a(t)}{dt} & = \lambda_a I_a(t) S(t) - (\theta_{ac} + \rho_a + \eta_C I_{aC}(t) + \mu_a) I_a(t) + \epsilon_2 I_a(t) dB_2(t) \\
\dfrac{dI_C(t)}{dt} & = \lambda_C I_C(t) S(t) - (\eta_a I_{aC}(t) + \rho_C + \mu_C) I_C(t) + \epsilon_3 I_C dB_3(t) \\
& \quad + \int_{\mathcal{U}} \Psi_2(u) I_C(s^-) \tilde{\mathcal{N}}(dt, du) \\
\dfrac{dI_{aC}(t)}{dt} & = (\eta_C I_a(t) + \eta_a I_C(t)) I_{aC}(t) - (\rho_{aC} + \theta_{acC} + \mu_{aC}) I_{aC})(t) \\
& \quad + \epsilon_4 I_{aC} dB_4(t) + \int_{\mathcal{U}} \Psi_3(u) I_{aC}(s^-) \tilde{\mathcal{N}}(dt, du) \\
\dfrac{dI_c(t)}{dt} & = \theta_{ac} I_a(t) + \phi_{cC} T_C - (\sigma_c + \mu_c) I_c(t) + \epsilon_5 I_c dB_5(t) \\
\dfrac{dI_{cC}(t)}{dt} & = \sigma_c I_c(t) + \theta_{acC} I_{aC} - (\mu_{cC} + \rho_{cC}) I_{cC}(t) + \epsilon_6 I_{cC} dB_6(t) \\
\dfrac{dT_a(t)}{dt} & = \rho_a I_a(t) - (\mu + \phi_a) T_a(t) + \epsilon_7 T_a dB_7(t) \\
\dfrac{dT_{aC}(t)}{dt} & = \rho_{aC} I_{aC}(t) - (\mu + \phi_{aC}) T_{aC}(t) + \epsilon_8 T_{aC} dB_8(t) \\
\dfrac{dT_C(t)}{dt} & = \rho_{cC} I_{cC}(t) + \rho_C I_C(t) - (\mu + \phi_C + \phi_{cC}) T_C(t) + \epsilon_9 T_C dB_9(t) \\
& \quad + \int_{\mathcal{U}} \Psi_4(u) T_C(s^-) \tilde{\mathcal{N}}(dt, du) \\
\dfrac{dR_a(t)}{dt} & = \phi_a T_a(t) - \mu R_a(t) + \epsilon_{10} R_a dB_{10}(t) \\
\dfrac{dR_{aC}(t)}{dt} & = \phi_{aC} T_{aC}(t) - (\mu + \sigma_{aC}) R_{aC}(t) + \epsilon_{11} R_{aC} dB_{11}(t) \\
\dfrac{dR_C(t)}{dt} & = \phi_C T_C(t) - (\mu + \sigma_C) R_C(t) + \epsilon_{12} R_C dB_{12}(t) \\
& \quad + \int_{\mathcal{U}} \Psi_5(u) R_C(s^-) \tilde{\mathcal{N}}(dt, du) \\
\dfrac{dV_C(t)}{dt} & = \theta_V S(t) - (\mu + \sigma_V) V_C(t) + \epsilon_{13} V_C dB_{13}(t),
\end{cases}
\tag{3}
$$

with initial conditions $S(0) > 0$, $I_C(0) \geq 0$, $I_a(0) \geq 0$, $I_{aC}(0) \geq 0$, $I_c(0) \geq 0$, $I_{cC}(0) \geq 0$, $T_a(0) \geq 0$, $T_C(0) \geq 0$, $T_{aC}(0) \geq 0$, $R_a(0) \geq 0$, $R_C(0) \geq 0$, $R_{aC}(0) \geq 0$, $V_C(0) \geq 0$.

The standard Brownian noise, $dB_i(t)$ is independent of $\tilde{\mathcal{N}}$. $\mathcal{N}$ is a Poisson counting measure with compensating martingale $\tilde{\mathcal{N}}$, v is a finite Lévy measure on a measurable subset $\mathcal{U} \in (0, \infty)$, where $v(\mathcal{U}) \leq \infty$. $v(\mathcal{U})$ describes the distribution of the random jump sizes in a Poisson-driven process. Again, since $\mathcal{U} \in (0, \infty)$, then every possible jump contributes to an increase and the expectation over $v(\mathcal{U})$ integrates over positive values, making its integral non-negative. $\tilde{\mathcal{N}} = \mathcal{N}(dt, du) - v(du)dt$. $\Psi_i : \mathcal{U} \to \Re$ $(i = 1, ..., 13)$ denotes the effects of random jumps and is bounded, and $\int_{\mathcal{U}} \Psi^2(X, s, u) v(du)$ is bounded. We also assume that $\int_{\mathcal{U}} (1 \wedge |x|^2) \nu(dx) < \infty$, thus, ensuring that the measure does not allow infinitely many jumps in a finite time interval.

We note that $S(t^-)$, $I_C(t^-)$, $I_a(t^-)$, $I_{aC}(t^-)$, $I_c(t^-)$, $I_{cC}(t^-)$, $T_a(t^-)$, $T_C(t^-)$, $T_{aC}(t^-)$, $R_a(t^-)$, $R_C(t^-)$, $R_{aC}(t^-)$ $V_C(t^-)$, denote the left limits of $S(t)$, $I_C(t)$, $I_a(t)$, $I_{aC}(t)$, $I_c(t)$, $I_{cC}(t)$, $T_a(t)$, $T_C(t)$, $T_{aC}(t)$, $R_a(t)$, $R_C(t)$, $R_{aC}(t)$, $V_C(t)$, respectively.

The following definitions are necessary for the analysis of the stochastic model.

Definition 1 (Itô-Lévy [67]). *First, set* $\Re^d_+ = \{\chi_i \in \Re^d_+, \chi > 0, d \geq 1\}$. *Suppose a complete probability space* $\big(\Omega, \mathcal{F}, P, \{\mathcal{F}_t\}_{t\geq 0}\big)$ *with filtration* $\{\mathcal{F}_t\}_{t\geq 0}$, *which satisfies the usual conditions of right-continuity and completeness.* $B_i(t)$ *is defined on this probability space. We assume an Itô -Lévy process,* $X(t) \in \Re^+$, *of the form*

$$dX(t) = F(X(t^-), t^-)dt + G(X(t^-), t^-)dB(t) + \int_{\mathcal{U}} \Psi(X(t^-), t^-, u)\tilde{\mathcal{N}}(dt, du), \tag{4}$$

with initial condition X(t=0) = X(0). $F : \Re^d \times \Re^+ \times S \to \Re^n$, $G : \Re^d \times \Re_+ \times S \to \Re^d$, *and* $\Psi : \Re^d \times \Re_+ \times S \times Y \to \Re^d$ *are measurable functions and* $X(t^-)$ *denotes the left limit of* $X(t)$. $F(X(t), t)$ *represents the linear drift term,* $G(X(t), t)$ *the Brownian noise,* $\tilde{\mathcal{N}}(dt, du)$ *represents the compensated Poisson random measure, and* $\Psi(X, t, u)$ *represents the intensity of jumps. It is assumed that (i)* $v(U)$ *is finite (i.e., the number of jumps in any finite interval is countable), (ii)* $\int_{\mathcal{U}}(1 \wedge |x|^2)\nu(dx) < \infty$, *(iii)*$|\Psi(X, s, u)| \leq C(1 + |X|)$, *where C is a constant,(iv)* $\int_{\mathcal{U}} \Psi^2(X, s, u)v(du) < \infty$, *and (v)* $\int_0^t \Big(|F(X, s)| + G^2(X, s) + \int_{\mathcal{U}} \Psi^2(X, s, u)v(du)\Big)ds < \infty$ *[67] are satisfied.*

Definition 2 (Itô-Lévy Formula [67]). *We consider the process X expressed by* (4) *and let* $\mathcal{V} \in C^{1,2}(\Re^d \times \Re^+ \times S; \Re_+)$ *such that* $\mathcal{Y} \equiv \mathcal{V}(t, X(t))$, *where* C^1 *means that the function is continuously differentiable with respect to time, and* C^2 *means that the function has continuous second-order partial derivatives with respect to the remaining variables.*

Then, $\mathcal{Y}(t)$ *is again an Itô-Lévy process and*

$$\begin{aligned} d\mathcal{Y}(t) = {} & \mathcal{V}_t(X, t)dt + \mathcal{V}_X(X, t)[F(X, t)dt + G(X, t)dB(t)] \\ & + \frac{1}{2} trace[G^T(X, t)\mathcal{V}_{XX}(X, t)G(X, t)]dt \\ & + \int_{\mathcal{U}} [\mathcal{V}(X + \Psi(X, t)) - \mathcal{V}(X, t) - \mathcal{V}_X(X, t)\Psi(X, t, u)]v(du)dt \\ & + \int_{\mathcal{U}} [\mathcal{V}(X + \Psi(X, t)) - \mathcal{V}(X, t)]\tilde{\mathcal{N}}(dt, du), \end{aligned}$$

which represents the generalized Itô's formula with jumps where

$$\mathcal{V}_t = \frac{\partial \mathcal{V}}{\partial t}, \ \mathcal{V}_X = \left(\frac{\partial \mathcal{V}}{\partial X_1}, \frac{\partial \mathcal{V}}{\partial X_2}, \ldots, \frac{\partial \mathcal{V}}{\partial X_n}\right), \ \mathcal{V}_{XX} = \left(\frac{\partial^2 \mathcal{V}}{\partial X_i \partial X_j}\right)_{d\times d}.$$

To gain insights into the underlying mechanisms that drive the spread of infectious diseases to identify the long-term behaviour of disease transmission we conduct qualitative analysis of the stochastic model (3).

3 Qualitative Analysis of Model

In this section, we present analysis on the existence of solution, positivity of the solution to (3), determine the reproductive number for single disease models and co-infection model, determine the conditions for Local and Global equilibrium for COVID-19 only, HBV only, and for co-infection model. Further we determine the conditions for extinction, and persistence for all three models.

3.1 Positivity of Model

Here, we determine the positivity of solution to the stochastic system (3) since a negative state will not be biologically meaningful. We will show the positivity of the solutions to (3). We proceed as follows

Theorem 1. *Let* $S(t^-)$, $I_C(t^-)$, $I_a(t^-)$, $I_{aC}(t^-)$, $I_c(t^-)$, $I_{cC}(t^-)$, $T_a(t^-)$, $T_C(t^-)$, $T_{aC}(t^-)$, $R_a(t^-)$, $R_C(t^-)$, $R_{aC}(t^-)$ $V_C(t^-)$, *denote the left limits of* $S(t)$, $I_C(t)$, $I_a(t)$, $I_{aC}(t)$, $I_c(t)$, $I_{cC}(t)$, $T_a(t)$, $T_C(t)$, $T_{aC}(t)$, $R_a(t)$, $R_C(t)$, $R_{aC}(t)$, $V_C(t)$ *be a solution of system* (3), *given initial values* $(S(0), I_C(0), I_a(0), I_{aC}(0), I_c(0), I_{cC}(0), T_a(0), T_C(0), T_{aC}(0), R_a(0), R_C(0), R_{aC}(0), V_C(0)) \in \Omega$, *where* $\Omega \in \Re^+$, *then* $\lim_{t\to\infty} S(t) \geq 0$, $\lim_{t\to\infty} I_C(t) \geq 0$, $\lim_{t\to\infty} I_a(t) \geq 0$, $\lim_{t\to\infty} I_{aC}(t) \geq 0$, $\lim_{t\to\infty} I_c(t) \geq 0$, $\lim_{t\to\infty} I_{cC}(t) \geq 0$, $\lim_{t\to\infty} T_a(t) \geq 0$, $\lim_{t\to\infty} T_C(t) \geq 0$, $\lim_{t\to\infty} T_{aC}(t) \geq 0$, $\lim_{t\to\infty} R_a(t) \geq 0$, $\lim_{t\to\infty} R_C(t) \geq 0$, $\lim_{t\to\infty} R_{aC}(t) \geq 0$, $\lim_{t\to\infty} V_C(t) \geq 0$.

Proof. We determine the positivity of the stochastic system (3). We proceed to show the positivity of the solution $S(t)$ to (3) as follows. We consider the first equation of (3),

$$\begin{aligned} dS(t) = [&\psi + \sigma_V V_C(t) + \sigma_{aC} R_{aC}(t) + \sigma_C R_C(t) - (\lambda_a I_a(t) + \lambda_C I_C(t))S(t) \\ &- (\mu + \theta_V)S(t)]dt + \epsilon_1 S(t) dB_1(t) + \int_{\mathcal{U}} \Psi_1(u) S(s^-) \tilde{\mathcal{N}}(dt, du). \end{aligned}$$

Eliminating first four terms on the right hand side and rearranging terms, we get

$$\begin{aligned} \frac{dS(t)}{S(t)} &\geq \Big[-(\lambda_a I_a(t) + \lambda_C I_C(t)) - (\mu + \theta_V) \Big] dt + \epsilon_1 dB_1(t) \\ &\quad + \int_{\mathcal{U}} \Psi_1(u) \tilde{\mathcal{N}}(dt, du) \\ &\geq -r dt + \epsilon_1 dB_1(t) + \mathcal{A} \end{aligned} \tag{5}$$

where $r = ((\lambda_a I_a(t) + \lambda_C I_C(t) + (\mu + \theta_V))$, and $\mathcal{A} = \int_{\mathcal{U}} \Psi_1(u) \tilde{\mathcal{N}}(dt, du)$. Next, we take a function $g(t, S(t)) = \ln(t, S(t))$ and apply Itô-Lévy formula in (18) to get

$$\begin{aligned} \int_0^t d \ln S(\kappa) d\kappa &\geq \int_0^t -r d\kappa + \int_0^t \epsilon_1 dB_1(\kappa) - \int_0^t \frac{1}{2}\epsilon_1^2 d\kappa + \int_0^t \mathcal{A} \\ &\geq \int_0^t -r d\kappa + \epsilon_1 \int_0^t dB_1(\kappa) - \frac{1}{2}\epsilon_1^2 \int_0^t d\kappa. \end{aligned}$$

Since $0 < \int_0^t \mathcal{A} < C < \infty$, where C is a positive constant, we have

$$\begin{aligned} \ln S(t) &\geq -rt + \epsilon_1 B_1(t) - \frac{1}{2}\epsilon_1^2 t + \ln S(0) \\ S(t) &\geq S(0) e^{-(r + \frac{1}{2}\epsilon_1^2)t + \epsilon_1 B_1(t)}. \end{aligned}$$

By taking the $\lim_{t\to\infty}$ on both sides we obtain

$$\lim_{t\to\infty} S(t) \geq \lim_{t\to\infty} S(0) e^{-(r + \frac{1}{2}\epsilon_1^2)t + \epsilon_1 B_1(t)} > 0.$$

It is clear that as $\lim_{t\to\infty}$, S(t) is positive definite.

Next, we show the positivity of the solution $I_a(t)$ to (3) as follows. We consider the first equation of (3)

$$dI_a(t) = [\lambda_a I_a(t)S(t) - (\theta_{ac} + \rho_a + \eta_C I_{aC}(t) + \mu_a)I_a(t)]dt + \epsilon_2 I_a(t)dB_2(t).$$

By eliminating first term on the right hand side and rearranging terms, we get

$$\begin{aligned} \frac{dI_a(t)}{I_a} &= [-(\theta_{ac} + \rho_a + \eta_C I_{aC}(t) + \mu_a)]dt + \epsilon_2(t)dB_2(t) \\ &= -rdt + \epsilon_2 dB_2(t), \end{aligned} \tag{6}$$

where $r = (\theta_{ac} + \rho_a + \eta_C I_{aC}(t) + \mu_a)$. Next, we take a function $g(t, I_a(t)) = \ln(t, I_a(t))$ and apply Itô's formula in [28] to get

$$\begin{aligned} d\ln I_a(t) &= \frac{1}{I_a}dI_a - \frac{1}{2I_a^2}(dI_a)^2 \\ &= \frac{1}{I_a}dI_a - \frac{1}{2I_a^2}(\epsilon_2 I_a dB)^2 \\ &= \frac{1}{I_a}dI_a - \frac{1}{2}(\epsilon_2^2 dt), \end{aligned}$$

where $dB^2 = dt$ (by quadratic variation of Brownian motion). A rearrangement yields

$$\frac{dI_a(t)}{I_a} = d\ln I_a(t) + \frac{1}{2}(\epsilon_2^2 dt). \tag{7}$$

Combining (6) and (7), integrating both sides and rearrangements gives

$$\begin{aligned} \int_0^t d\ln I_a(\kappa)d\kappa &\geq \int_0^t -rd\kappa + \int_0^t \epsilon_2 dB_2(\kappa) - \int_0^t \frac{1}{2}\epsilon_2^2 d\kappa \\ &\geq \int_0^t -rd\kappa + \epsilon_2 \int_0^t dB_2(\kappa) - \frac{1}{2}\epsilon_2^2 \int_0^t d\kappa \\ \ln I_a(t) &\geq -rt + \epsilon_2 B_2(t) - \frac{1}{2}\epsilon_2^2 t + \ln I_a(0) \\ I_a(t) &\geq I_a(0)e^{-(r+\frac{1}{2}\epsilon_2^1)t+\epsilon_2 B_2(t)}. \end{aligned}$$

Taking the $\lim_{t\to\infty}$ on both sides we obtain

$$\lim_{t\to\infty} I_a(t) \geq \lim_{t\to\infty} I_a(0)e^{-(r+\frac{1}{2}\epsilon_2^2)t+\epsilon_2 B_2(t)} > 0.$$

Hence $I_a(t)$ is positive definite.

We can show using similar approach that, $\lim_{t\to\infty} I_C(t) > 0, \lim_{t\to\infty} I_{aC}(t) > 0, \lim_{t\to\infty} I_c(t) > 0, \lim_{t\to\infty} I_{cC}(t) > 0, \lim_{t\to\infty} T_a(t) > 0, \lim_{t\to\infty} T_C(t) > 0, \lim_{t\to\infty} T_{aC}(t) > 0, \lim_{t\to\infty} R_a(t) > 0, \lim_{t\to\infty} R_C(t) > 0, \lim_{t\to\infty} R_{aC}(t) > 0, \lim_{t\to\infty} V_C(t) > 0.$ □

3.2 Invariant Region of Stochastic COVID-19 and Hepatitis B co-infection Model

An investigation of the invariant region of the model will help us determine the set of states for which the disease will eventually either persist or die out infinitely.

Theorem 2. *Let* $N(t) = S(t)+I_C(t)+I_a(t)+I_{aC}(t)+I_c(t)+I_{cC}(t)+T_a(t)+T_C(t)+T_{aC}(t)+R_a(t)+R_C(t)+R_{aC}(t)+V_C(t)$ *be the population of system* (3)*, then* $N(t)$ *is invariant over time, that is* $0 < \lim_{t\to\infty} N(t) \leq \frac{\psi}{\mu}$*, and* $(S(0), I_C(0), I_a(0), I_{aC}(0), I_c(0), I_{cC}(0), T_a(0), T_C(0), T_{aC}(0), R_a(0), R_C(0), R_{aC}(0),$
$V_C(0)) \in \Omega$.

Proof. From (1), we know that

$$\begin{aligned} N(t) = S(t) + I_C(t) + I_a(t) + I_{aC}(t) + I_c(t) + I_{cC}(t) + T_a(t) \\ + T_C(t) + T_{aC}(t) + R_a(t) + R_C(t) + R_{aC}(t) + V_C(t). \end{aligned}$$

By differentiating (1) we obtain

$$\begin{aligned} \frac{dN(t)}{dt} = \frac{dS(t)}{dt} + \frac{I_C(t)}{dt} + \frac{I_a(t)}{dt} + \frac{I_{aC}(t)}{dt} + \frac{I_c(t)}{dt} + \frac{I_{cC}(t)}{dt} + \frac{T_a(t)}{dt} \\ + \frac{T_C(t)}{dt} + \frac{T_{aC}(t)}{dt} + \frac{R_a(t)}{dt} + \frac{R_C(t)}{dt} + \frac{R_{aC}}{dt} + \frac{V_C(t)}{dt}. \end{aligned}$$

Substituting the derivatives and simplifying terms in (3) we obtain

$$\begin{aligned} dN(t) = \psi + \sigma_V V_C(t) + \sigma_{aC} R_{aC}(t) + \sigma_C R_C(t) - (\lambda_a I_a(t) + \lambda_C I_C(t))S(t) \\ - (\mu + \theta_V)S(t) + \lambda_a I_a(t)S(t) - (\theta_{ac} I_a(t) + \rho_a + \eta_C I_{aC}(t) + \mu_a)I_a(t) \\ + \lambda_C I_C(t)S(t) - (\eta_a I_{aC}(t) + \rho_C + \mu_C)I_C(t) + (\eta_C I_a(t) \\ + \eta_a I_C(t))I_{aC}(t) - (\rho_{aC} + \theta_{acC} + \mu_{aC})I_{aC})(t) + \theta_{ac} I_a(t) + \phi_{cC} T_C \\ - (\sigma_c + \mu_c)I_c(t) + \sigma_c I_c(t) + \theta_{acC} I_{aC} - (\mu_{cC} + \rho_{cC})I_{cC}(t) + \rho_a I_a(t) \\ - (\mu + \phi_a)T_a(t) + \rho_{aC} I_{aC}(t)(\mu + \phi_{aC})T_{aC}(t) + \rho_{cC} I_{cC}(t) + \rho_C I_C(t) \\ - (\mu + \phi_C + \phi_{cC})T_C(t) + \phi_a T_a(t) - \mu R_a(t) + \phi_{aC} T_{aC}(t) - (\mu + \sigma_{aC}) \\ \times R_{aC}(t) + \phi_C T_C(t) - (\mu + \sigma_C)R_C + \theta_V S(t) - (\mu + \sigma_V)V_C(t) \\ + \epsilon_1 S(t)dB_1(t) + \epsilon_2 I_a(t)dB_2(t) + \epsilon_3 I_C dB_3(t) + \epsilon_4 I_{aC} dB_4(t) \\ + \epsilon_5 I_c dB_5(t) + \epsilon_6 I_{cC} dB_6(t) + \epsilon_7 T_a dB_7(t) + \epsilon_8 T_{aC} dB_8(t) + \epsilon_9 T_C dB_9(t) \\ + \epsilon_{10} R_a dB_{10}(t) + \epsilon_{11} R_{aC} dB_{11}(t) + \epsilon_{12} R_C dB_{12}(t) + \epsilon_{13} V_C dB_{13}(t) \\ + \int_{\mathcal{U}} \Psi_1(u)S(t)(s^-)\tilde{\mathcal{N}}(dt, du) + \int_{\mathcal{U}} \Psi_2(u)I_C(s^-)\tilde{\mathcal{N}}(dt, du) \\ + \int_{\mathcal{U}} \Psi_3(u)I_{aC}(s^-)\tilde{\mathcal{N}}(dt, du) + \int_{\mathcal{U}} \Psi_4(u)T_C(s^-)\tilde{\mathcal{N}}(dt, du) \\ + \int_{\mathcal{U}} \Psi_5(u)R_C(s^-)\tilde{\mathcal{N}}(dt, du). \end{aligned} \tag{8}$$

We let $\mu_a = \mu_{aC} = \mu_c = \mu_{cC} = \mu_C = \mu$ and choose $\epsilon = \max(\epsilon_1, \epsilon_2, \epsilon_3, \epsilon_4, \epsilon_5, \epsilon_6, \epsilon_7, \epsilon_8, \epsilon_9, \epsilon_{10}, \epsilon_{11}, \epsilon_{12}, \epsilon_{13})$ and $(\nabla_1, \nabla_2, \nabla_3, \nabla_4, \nabla_5) = (S, I_C, I_{aC}, T_C, R_C)$ to obtain

$$\begin{aligned} dN(t) &\leq (\psi - \mu N(t))dt + \epsilon N(t)dB(t) + \int_{\mathcal{U}} \sum_{i=1}^{5} \Psi_i(u)\nabla_i(t^-)\tilde{\mathcal{N}}(dt, du) \\ &\leq (\psi - \mu N(t))dt + \epsilon N(t)dB(t) + \int_{\mathcal{U}} \Psi N(t^-)\tilde{\mathcal{N}}(dt, du). \end{aligned} \tag{9}$$

with $N(0) > 0$. (9) satisfies the Itô- Lévy process. By rearrangement of (9) we obtain a non-homogeneous differential equation. Next, we determine the homogeneous and particular solution and obtain the general solution to equation (9) as

$$N(t) \leq N(0)e^{-(\mu+\frac{1}{2}\epsilon^2)t+\epsilon B(t)+\int_0^t\int_{\mathcal{U}}\ln(1+\Psi(u)\tilde{\mathcal{N}}(ds,du))} + \frac{\psi}{\mu}.$$

By taking the limit, we finally obtain the solution to (9) as,

$$\lim_{t\to\infty} N(t) \leq \lim_{t\to\infty} N(0)e^{-(\mu t+\frac{1}{2}\epsilon^2)t+\epsilon B(s)+\int_0^t\int_{\mathcal{U}}\ln(1+\Psi(u)\tilde{\mathcal{N}}(ds,du))} + \lim_{t\to\infty}\frac{\psi}{\mu},$$

$$0 < \lim_{t\to\infty} N(t) \leq \frac{\psi}{\mu}.$$

□

3.3 Disease Free Equilibrium Point

We consider the first equation of (3). For disease free equilibrium, we have $I_a(t) = 0, I_C(t) = 0, I_{aC}(t) = 0, I_{CC}(t) = 0, T_C(t) = 0, T_a(t), R_C(t) = 0, R_a(t) = 0, R_{aC}(t) = 0, V(t) = 0$. We let $\frac{dS(t)}{dt} = 0$,

$$\psi - \mu S(t) + \epsilon_1 S(t)dB_1 + \int_{\mathcal{U}} \Psi_1(u)S(t^-)\tilde{\mathcal{N}}(dt,du) = 0.$$

Next, we solve for $S(t)$ as

$$S(t) = \frac{\psi}{\mu + \epsilon_1(dB_1) + \int_{\mathcal{U}}\Psi_1(u)\tilde{\mathcal{N}}(dt,du)} \leq \frac{\psi}{\mu}.$$

We find the expectation $\mathbb{E}(S(t))$ to get

$$\mathbb{E}(S(t)) = \frac{\psi}{\mu + \epsilon_1\mathbb{E}(dB_1) + \mathbb{E}\int_{\mathcal{U}}\Psi_1(u)\tilde{\mathcal{N}}(dt,du)} \leq \frac{\psi}{\mu}.$$

The above result is obtained by applying Definition 1 and comparison [51]. Hence, the disease free equilibrium is given by

$$\begin{aligned} E_{0HC} &= (S(t), I_C(t), I_a(t), I_{aC}(t), I_c(t), I_{cC}(t), T_a(t), T_C(t), T_{aC}(t), R_a(t), \\ &\quad R_C(t), R_{aC}(t), V_C(t)) \\ &= \left(\frac{\psi}{\mu}, 0, 0, 0, 0, 0, 0, 0, 0, 0, 0, 0, 0\right). \end{aligned} \tag{10}$$

3.4 Reproductive Number for COVID-19 only Model

The reproduction number, $\mathcal{R}_0$ of a disease determines the average number of secondary infections when an infectious person is introduced into in a completely susceptible population. It is therefore an important parameter in disease control. In this section we present results on the Reproductive Number for the deterministic COVID-19 model, $\mathcal{R}^d_{0C}$, and the reproductive number for the COVID-19 model in the stochastic sense $\mathcal{R}^s_{0C}$. Next we determine stability conditions for $\mathcal{R}^d_{0C}$, and $\mathcal{R}^s_{0C}$ respectively.

3.4.1 Basic Reproductive Number of Deterministic COVID-19 Only Model

To obtain the basic reproduction number, we consider the infected class of COVID-19 deterministic model given by

$$\begin{cases} \dfrac{dS(t)}{dt} & = \psi + \sigma_V V_C(t) + \sigma_C R_C(t) - \lambda_C I_C(t) S(t) \\ & \quad -(\mu + \theta_V) S(t) \\ \dfrac{dI_C(t)}{dt} & = \lambda_C I_C(t) S(t) - (\rho_C + \mu_C) I_C(t) \\ \dfrac{dT_C(t)}{dt} & = \rho_C I_C(t) - (\mu + \phi_C) T_C(t) \\ \dfrac{dR_C(t)}{dt} & = \phi_C T_C(t) - (\mu + \sigma_C) R_C(t) \\ \dfrac{dV_C(t)}{dt} & = \theta_V S(t) - (\mu + \sigma_V) V_C(t), \end{cases} \tag{11}$$

with initial conditions $S(0) > 0$, $I_C(0) \geq 0$, $T_C(0) \geq 0$, $R_C(0) \geq 0$, $V_C(0) \geq 0$. We employ the Next Generation Matrix (NGM) method , see, e.g., [9] to determine the basic reproductive number of the deterministic model. When using the NGM method , the basic reproductive number is defined as the spectra radius (largest eigenvalue) of $FV^{-}1$, where F and V are the partial derivatives of f, and V respectively, and f and v are the matrices of initial infections and secondary infections respectively. The inverse of V, V^{-1} is defined as

$$V^{-1} = \frac{1}{detV}(adjV).$$

We therefore proceed by considering the primary or initial infections f and secondary infections v of infectious states of (11). The primary infections f is given as

$$f = \lambda_C I_C S = \frac{\beta_C(1 - \kappa\zeta) I_C(t) S(t)}{N}$$

and the secondary infections v is given by

$$v = (\rho_C + \mu_C) I_C(t).$$

Finding the partial derivative of f and v with respect to $I_C(t)$ and evaluating at DFE we get

$$\begin{aligned} F &= \frac{\beta_C(1 - \kappa\zeta) S(t)}{N} \\ &= \beta_C(1 - \kappa\zeta) \end{aligned}$$

and

$$V = (\rho_C + \mu_C).$$

Multiplying F and V^{-1}, we get

$$FV^{-1} = \frac{\beta_C(1 - \kappa\zeta)}{(\rho_C + \mu_C)}.$$

Taking the spectral radius of FV^{-1}, i.e., $\rho(FV^{-1})$, we obtain

$$\mathcal{R}_{0C}^d = FV^{-1} = \frac{\beta_C(1 - \kappa\zeta)}{(\rho_C + \mu_C)}. \tag{12}$$

Hence the deterministic reproductive number of COVID-19 only transmission is $\mathcal{R}_{0C}^d$.

3.4.2 Basic Reproductive Number of Stochastic COVID-19 Only Model

Next, we determine the reproduction number of the COVID-19 stochastic model. We recall to the COVID-19 infected class of (3).

$$\begin{aligned} dI_C(t) &= (\lambda_C I_C(t)S(t) - (\rho_C + \mu_C)I_C(t))dt + \epsilon_3 I_C(t)dB_3(t) \\ &\quad + \int_{\mathcal{U}} \Psi_2(u) I_C(s^-)\tilde{\mathcal{N}}(dt, du). \end{aligned} \tag{13}$$

We set a function $g(t, I_C(t)) = \ln(t, I_C(t))$ and apply Itô- Lévy formula, and evaluate at DFE to get

$$\begin{aligned} d\ln I_C(t) &= \Big[\lambda_C S(t) - (\rho_C + \mu_C) - \frac{\epsilon_3^2}{2} - \int_{\mathcal{U}} (\Psi_2(u) - \ln(1 + \Psi_2(u)))v(du)\Big]dt \\ &\quad + \epsilon_3 dB_3(t) + \int_{\mathcal{U}} (\ln(1 + \Psi_2(u))\tilde{\mathcal{N}}(dt, du) \\ &= \Big[\beta_C(1 - \kappa\zeta) - (\rho_C + \mu_C) - \frac{\epsilon_3^2}{2} - \int_{\mathcal{U}} (\Psi_2(u) - \ln(1 + \Psi_2(u)))v(du)\Big]dt \\ &\quad + \epsilon_3 dB_3(t) + \int_{\mathcal{U}} (\ln(1 + \Psi_2(u))\tilde{\mathcal{N}}(dt, du). \end{aligned} \tag{14}$$

Considering partial derivatives of initial infections F and secondary infections V, we determine the basic reproduction number by means of the next generation matrix [9] as follows

$$F = \beta_C(1 - \kappa\zeta) - \frac{1}{2}\epsilon_3^2 - \int_{\mathcal{U}} (\Psi_2(u) - \ln(1 + \Psi_2(u)))v(du),$$

and

$$V = \rho_C + \mu_C.$$

By multiplying F and V^{-1} and factorising $(\rho_C + \mu_C)$ we obtain

$$FV^{-1} = (\rho_C + \mu_C)^{-1}\Big(\beta_C(1 - \kappa\zeta) - \frac{1}{2}\epsilon_3^2 - \int_{\mathcal{U}} (\Psi_2(u) - \ln(1 + \Psi_2(u)))v(du)\Big).$$

Taking the spectral radius of FV^{-1}, i.e., $\rho(FV^{-1})$, we obtain

$$\mathcal{R}_{0C}^s = \rho(FV^{-1}) = \frac{\beta_C(1 - \kappa\zeta)}{(\rho_C + \mu_C)} - \frac{\epsilon_3^2}{2(\rho_C + \mu_C)} - \frac{\int_{\mathcal{U}} (\Psi_2(u) - \ln(1 + \Psi_2(u)))v(du)}{(\rho_C + \mu_C)}. \tag{15}$$

Next we examine the local stability of the $\mathcal{R}_{0C}^d$ at DFE.

3.4.3 Local Stability of Deterministic COVID-19 Only Model

Theorem 3. *The COVID-19 disease free equilibrium point is locally asymptotically stable if and only if $\mathcal{R}_{0C}^d < 1$ and unstable otherwise.*

Proof. The Jacobian matrix of model (11) is given as

$$J = \begin{pmatrix} -\lambda_C I(t) - (\mu + \theta_V) & -\lambda_C S(t) & 0 & \sigma_C & \sigma_V \\ \lambda_C I(t) & \lambda_C S(t) - \mu_C - \rho_C & 0 & 0 & 0 \\ 0 & \rho_C & -\mu - \phi_C & 0 & 0 \\ 0 & 0 & \phi_C & -\mu - \sigma_C & 0 \\ \theta_V & 0 & 0 & 0 & -\mu - \sigma_V \end{pmatrix} \tag{16}$$

We solve (31) at the disease free equilibrium point and obtain

$$J(E_{0C}) = \begin{pmatrix} -(\mu+\theta) & -\beta_C & 0 & \sigma_C & \sigma_V \\ 0 & \beta_C(1-\kappa\zeta)-\mu_C-\rho_C & 0 & 0 & 0 \\ 0 & \rho_C & -\mu-\phi_C & 0 & 0 \\ 0 & 0 & \phi_C & -\mu-\sigma_C & 0 \\ \theta & 0 & 0 & 0 & -\mu-\sigma_V \end{pmatrix} \tag{17}$$

Next, we determine the characteristic matrix by $\det(J(E_{0C})-\lambda I)$ where I is the identity matrix. The corresponding characteristic equation is given as

$$y = (-\mu-\lambda)(-(\mu+\sigma_V+\theta_V)-\lambda)(-(\mu+\sigma_C)-\lambda)(-(\mu+\phi_C)-\lambda)(\beta_C-(\mu_C+\rho_C)-\lambda).$$

By letting $\det(J-\lambda I)=0$, we observe that the three eigenvalues $\lambda_1=-\mu, \lambda_2=-(\mu+\sigma_V+\theta_V), \lambda_3=-(\mu+\sigma_C), \lambda_4=-(\mu+\phi_C)$ are negative, since all parameters are non-negative. However, for stability, all real parts of the eigenvalues must be negative. This implies

$$\begin{aligned} (\beta_C(1-\kappa\zeta)-(\mu_C+\rho_C) &< 1 \\ \frac{\beta_C(1-\kappa\zeta)}{(\mu_C+\rho_C)} &< 0 \\ \mathcal{R}^d_{0C} &< 1. \end{aligned}$$

□

3.4.4 Local Stability of Stochastic COVID-19 Only Model

It is crucial to understand the behaviour of a dynamical system near the disease-free equilibrium point. Checking for local stability at this point helps to determine whether small introductions of the COVID-19 will lead to extinction or an outbreak of the disease.

Theorem 4. *If $\mathcal{R}^s_{0C}<1$, then for any initial values of $(S(0), I_C(0), T_C(0), R_C(0), V_C(0)) \in \Re^5_+$, $I_C(t)$ satisfies $\limsup_{t\to\infty} \frac{\ln I_C(t)}{t} \leq 0$.*

Proof. We recall (18), the Itô- Lévy expression for the COVID-19 infected class of (3).

$$\begin{aligned} d\ln I_C(t) = &\Big[\lambda_C S(t)-(\rho_C+\mu_C)-\frac{\epsilon_3^2}{2}-\int_{\mathcal{U}}(\Psi_2(u)-\ln(1+\Psi_1(u)))v(du)\Big]dt \\ &+\epsilon_3 dB_3(t)+\int_{\mathcal{U}}(\ln(1+\Psi_2(u))\tilde{\mathcal{N}}(dt,du) \end{aligned} \tag{18}$$

By integrating both sides of (18) and evaluating at disease free-equilibrium point, we have

$$\begin{aligned} \ln I_C(t)-\ln I_C(0) &= \lambda_C\int_0^t S(r)dr-\Big(\rho_C+\mu_C+\frac{\epsilon_3^2}{2}\Big)t+\int_0^t \epsilon_3 dB_3(r) \\ &\quad -t\int_{\mathcal{U}}(\Psi_2(u) \quad -\ln(1+\Psi_2(u)))v(du) \\ &\quad +\int_0^t\int_{\mathcal{U}}\ln(1+\Psi_2(u))\tilde{\mathcal{N}}(ds,du) \\ &= \left[\frac{\beta_C(1-\kappa\zeta)\mu\psi}{\mu\psi}-(\rho_C+\mu_C)-\frac{\epsilon_3^2}{2})-\mathcal{E}_1\right]t+\mathcal{H}_1(t)+\mathcal{A}_1, \end{aligned}$$

where $\mathcal{H}_1(t) = \int_0^t \epsilon_3 dB_3(t)$, $\mathcal{E}_1 = \int_{\mathcal{U}}(\Psi_2(u) - \ln(1+\Psi_2(u)))v(du)$, and $\mathcal{A}_1 = \int_0^t \int_{\mathcal{U}} \ln(1+\Psi_2(u))\tilde{\mathcal{N}}(ds,du)$ are martingales given $\int_{\mathcal{U}} \ln(1+\Psi_2(u))\tilde{\mathcal{N}}(dt,du) < \infty$, $0 \le t \le T$.
Next, we divide through by t, take $\limsup_{t\to\infty}$ of both sides, and apply Lemma (1) to get,

$$\begin{aligned}
\limsup_{t\to\infty} \frac{\ln I_C(t)}{t} &= \limsup_{t\to\infty} \frac{\ln I_C(0)}{t} + \left[\beta_C(1-\kappa\zeta) - (\rho_C+\mu_C) - \frac{\epsilon_3^2}{2} - \mathcal{E}_1\right] \\
&\quad + \limsup_{t\to\infty} \frac{\mathcal{H}_1(t)}{t} + \limsup_{t\to\infty} \frac{\mathcal{A}_1}{t} \\
&= (\rho_C+\mu_C)\Big[\frac{\beta_C(1-\kappa\zeta)}{(\rho_C+\mu_C)} - 1 - \frac{\epsilon_3^2}{2(\rho_C+\mu_C)} - \frac{\mathcal{E}_1}{(\rho_C+\mu_C)}\Big] \\
&= (\rho_C+\mu_C)\left(\mathcal{R}_{0C}^s - 1\right).
\end{aligned}$$

For

$$\limsup_{t\to\infty} \frac{\ln I_C(t)}{t} = (\rho_C+\mu_C)\left(\mathcal{R}_{0C}^s - 1\right) < 0,$$

$$\mathcal{R}_{0C}^s - 1 < 0,$$

since

$$(\rho_C+\mu_C) > 0.$$

This implies that whenever $\mathcal{R}_{0C}^s < 1$, $\limsup_{t\to\infty} \dfrac{\ln I_C(t)}{t} \le 0$. □

3.4.5 Global Stability of Stochastic COVID-19 Only Model

Theorem 5. *If $\mathcal{R}_{0C}^s < 1$, then E_{0C} is globally asymptotically stable in Ω.*

Proof. We consider a Lyapunov function $L_1(t)$, see, e.g., [45],

$$L_1(t) = \left[\psi + \alpha\delta + \frac{\psi\theta}{\mu\delta}\right] I_C(t). \tag{19}$$

We differentiate (19), substitute (13), and evaluate at DFE to get

$$\begin{aligned}
\frac{dL_1}{dt} &= \left[\psi + \alpha\delta + \frac{\psi\theta}{\mu\delta}\right]\Big((\lambda_C S(t) - (\eta_a I_{aC}(t) + \rho_C + \mu_C)) + \epsilon_3 dB_3(t) \\
&\quad + \int_{\mathcal{U}} \Psi_2(u)(s^-)\tilde{\mathcal{N}}(dt,du)\Big) I_C(t) \\
&= \left[\psi + \alpha\delta + \frac{\psi\theta}{\mu\delta}\right](\rho_C+\mu_C)\Big[\frac{\beta_C(1-\kappa\zeta)}{(\rho_C+\mu_C)} - 1 + \frac{\epsilon_3 dB_3(t)}{(\rho_C+\mu_C)} \\
&\quad + \frac{1}{(\rho_C+\mu_C)}\mathbb{B}_1\Big] I_C(t),
\end{aligned}$$

where $\mathbb{B}_1 = \int_{\mathcal{U}} \Psi_2(u)\tilde{\mathcal{N}}(dt,du)$, and $\mathcal{E}_1 = \int_{\mathcal{U}}(\Psi_2(u) - \ln(1+\Psi_2(u)))v(du)$.
Clearly

$$\left[\psi + \alpha\delta + \frac{\psi\theta}{\mu\delta}\right](\rho_C+\mu_C) > 0.$$

For

$$\frac{dL_1}{dt} < 0,$$

$$\Big[\frac{\beta_C(1-\kappa\zeta)}{(\rho_C+\mu_C)} - 1 + \frac{\epsilon_3 dB_3(t)}{(\rho_C+\mu_C)} + \frac{\mathbb{B}_1}{(\rho_C+\mu_C)}\Big] < 0.$$

By comparison we obtain

$$\Big[\frac{\beta_C(1-\kappa\zeta)}{(\rho_C+\mu_C)} - 1 - \frac{\epsilon_3^2}{2(\rho_C+\mu_C)} - \frac{\mathcal{E}_1}{(\rho_C+\mu_C)}\Big] \quad <$$
$$\Big[\frac{\beta_C(1-\kappa\zeta)}{(\rho_C+\mu_C)} - 1 + \frac{\epsilon_3 dB_3(t)}{(\rho_C+\mu_C)} + \frac{\mathbb{B}_1}{(\rho_C+\mu_C)}\Big] < 0,$$

From (15) we conclude

$$\mathcal{R}_{0C}^s - 1 < 0$$
$$\mathcal{R}_{0C}^s < 1.$$

Hence, L_1 is globally stable in the domain Ω. □

3.5 Basic Reproductive Number for HBV Only Model

In this section we present results on the Reproductive Number for the deterministic reproductive number of the HBV only model, $\mathcal{R}_{0a}^d$, and the reproductive number of the HBV only model in the stochastic sense $\mathcal{R}_{0a}^s$. Next we determine stability conditions for $\mathcal{R}_{0a}^d$, and $\mathcal{R}_{0a}^s$ respectively.

3.5.1 Basic Reproductive Number of Deterministic HBV Only Model

To obtain the basic reproduction number, we consider the infected class of HBV deterministic model given by

$$\begin{cases} \dfrac{dS(t)}{dt} & = \psi - \lambda_a I_a(t)S(t) - \mu S(t) + \epsilon_1 S(t)dB_1(t) \\ \dfrac{dI_a(t)}{dt} & = \lambda_a I_a(t)S(t) - (\rho_a + \mu_a + \theta_{ac})I_a(t) \\ \dfrac{dI_c(t)}{dt} & = \theta_{ac} I_a(t) - \mu_c I_c(t) \\ \dfrac{dT_a(t)}{dt} & = \rho_a I_a(t) - (\mu + \phi_a)T_a(t) \\ \dfrac{dR_a(t)}{dt} & = \phi_a T_a(t) - \mu R_a(t), \end{cases} \tag{20}$$

with initial conditions $S(0) > 0$, $I_a(0) \geq 0$, $I_c(0) \geq 0$, $T_a(0) \geq 0$, $R_a(0) \geq 0$.

We employ the next generation matrix [9] method described earlier to determine the basic reproductive number of the deterministic model. We proceed by considering the primary or initial infections f and secondary infections v of (11)

$$f = \begin{pmatrix} \lambda_a I_a S(t) \\ 0 \end{pmatrix} \tag{21}$$

$$v = \begin{pmatrix} (\rho_a + \mu_a + \theta_{ac})I_a(t) \\ \theta_{ac} I_a(t) - \mu_c I_c(t) \end{pmatrix}. \tag{22}$$

Finding the partial derivative of f and v with respect to $I_C(t)$ and evaluating at DFE gives,

$$F = \begin{pmatrix} \beta_a(1-\kappa\zeta) & 0 \\ 0 & 0 \end{pmatrix} \tag{23}$$

and

$$V = \begin{pmatrix} (\rho_a + \mu_a + \theta_{ac}) & 0 \\ 0 & \mu_c \end{pmatrix}. \tag{24}$$

The inverse of V is obtained as

$$V^{-1} = \begin{pmatrix} \dfrac{1}{(\rho_a + \mu_a + \theta_{ac})} & 0 \\ 0 & \dfrac{1}{\mu_c} \end{pmatrix}. \tag{25}$$

Multiplying F and V^{-1}, we get

$$FV^{-1} = \begin{pmatrix} \dfrac{\beta_a(1-\kappa\zeta)}{(\rho_a + \mu_a + \theta_{ac})} & 0 \\ 0 & 0 \end{pmatrix} \tag{26}$$

Taking the spectral radius of FV^{-1}, i.e., $\rho(FV^{-1})$, we obtain

$$\mathcal{R}_{0a}^d = FV^{-1} = \frac{\beta_a(1-\kappa\zeta)}{(\rho_a + \mu_a + \theta_{ac})}. \tag{27}$$

Next, we determine the reproduction number of the HBV stochastic model.

3.5.2 Basic Reproductive Number for Stochastic HBV Only Model

We consider the acute HBV infectious state of the HBV only stochastic sub-model

$$dI_a(t) = (\lambda_a I_a(t)S(t) - (\rho_a + \mu_a + \theta_{ac})I_a(t))dt + \epsilon_2 I_a(t)dB_2(t). \tag{28}$$

Next, we take a function $g(t, I_a(t)) = \ln(t, I_a(t))$. Applying Itô- Lévy formula to the HBV infected class of (28), we obtain

$$d\ln I_a(t) = \big(\lambda_a S(t) - (\rho_a + \mu_a + \theta_{ac}) - \frac{\epsilon_2^2}{2}\big)dt + \epsilon_2 dB_2(t). \tag{29}$$

Next, we employ the next generation matrix [9] method to determine the basic reproductive number of the deterministic model. The partial derivatives with respect to I_a of the initial infections F and of secondary infections V are obtained and evaluated at DFE as follows

$$F = \lambda_a S(t) - \frac{1}{2}\epsilon_2^2$$
$$F|_{DFE} = \frac{\beta_a(1-\kappa\zeta)\psi\mu}{\mu\psi} - \frac{1}{2}\epsilon_2^2,$$

and

$$V = \rho_a + \mu_a$$
$$V^{-1} = \frac{1}{\alpha + \mu + \rho_c}.$$

By multiplying F and V^{-1} we get

$$FV^{-1} = \frac{\beta_a(1-\kappa\zeta)}{(\rho_a + \mu_a + \theta_{ac})} - \frac{\epsilon_2^2}{2(\rho_a + \mu_a + \theta_{ac})}.$$

Taking the spectral radius of FV^{-1}, i.e., $\rho(FV^{-1})$, we obtain

$$\mathcal{R}_{0a}^s = \rho(FV^{-1}) = \frac{\beta_a(1-\kappa\zeta)}{\rho_a + \mu_a + \theta_{ac}} - \frac{\epsilon_2^2}{2(\rho_a + \mu_a + \theta_{ac})}. \tag{30}$$

3.5.3 Local Stability of Deterministic HBV Only Model

Theorem 6. *The HBV disease free equilibrium point is locally asymptotically stable if and only if* $\mathcal{R}_{0a}^{d} < 1$ *and unstable otherwise.*

Proof. The Jacobian matrix of model (20) is given as

$$J = \begin{pmatrix} -\lambda_a I_a(t) - \mu & -\lambda_a S(t) & 0 & 0 & 0 \\ \lambda_a I_a(t) & \lambda_a S(t) - \mu_a - \rho_a - \theta_{ac} & 0 & 0 & 0 \\ 0 & \theta_{ac} & -\mu_c & 0 & 0 \\ 0 & \rho_a & 0 & -\mu - \phi_a & 0 \\ 0 & 0 & 0 & \phi_a & -\mu \end{pmatrix}. \tag{31}$$

We solve (31) at the disease free equilibrium point and obtain

$$J(E_{0C}) = \begin{pmatrix} -\mu & -\beta_a & 0 & 0 & 0 \\ 0 & \beta_C(1-\delta\zeta) - \mu_a - \rho_a - \theta_{ac} & 0 & 0 & 0 \\ 0 & \theta_{ac} & -\mu_c & 0 & 0 \\ 0 & \rho_a & 0 & -\mu - \phi_a & 0 \\ 0 & 0 & 0 & \phi_a & -\mu \end{pmatrix}. \tag{32}$$

Next, we determine the characteristic matrix by $\det(J(E_{0C}) - \lambda I)$ where I is the identity matrix. The corresponding characteristic equation is given as

$$(-\mu_c - \lambda), (-\mu - \phi_a) - \lambda), ((\beta_a(1-\kappa\zeta) - \mu_a - \rho_a - \theta_{ac}) - \lambda), (-\mu - \lambda), (-\mu - \lambda).$$

By letting $\det(J - \lambda I) = 0$, we observe that the three eigenvalues $\lambda_1 = -\mu_c, \lambda_2 = -(\phi_a + \mu), \lambda_4 = -\mu, \lambda_5 = -\mu$ are negative, since all parameters are non-negative. However, for stability, all real parts of the eigenvalues must be negative. This implies

$$\begin{aligned} \big(\beta_a(1-\kappa\zeta) - (\mu_a + \rho_a + \theta_{ac})\big) &< 0 \\ \frac{\beta_a(1-\kappa\zeta)}{(\mu_a + \rho_a + \theta_{ac})} &< 1 \\ \mathcal{R}_{0a}^{d} &< 1. \end{aligned}$$

□

3.5.4 Local Stability of Stochastic HBV Only Model

Local stability analysis at disease-free equilibrium point helps determine whether the introduction of a few infected HBV individuals in the population will become extinct or lead to an outbreak. This is crucial for understanding the behaviour of a dynamical system near that point in the presence of minor disturbances.

Theorem 7. *If* $\mathcal{R}_{0a}^{s} < 1$*, then for any initial values of* $(S(0), I_a(0), I_c(0), T_a(0), R_a(0)) \in \Re_{+}^{5}$*,* $I_a(t)$ *satisfies* $\limsup_{t\to\infty} \frac{\ln I_a(t)}{t} \leq 0$.

Proof. We recall (28). By setting a function $g(t, I_a(t)) = \ln(t, I_a(t))$ and applying Itô formula to (28), we obtain (29). We integrate both sides of (29) and evaluate at DFE point to obtain

$$\begin{aligned}\ln I_a(t) &= \ln I_a(0) + \left[\lambda_a S(t) - (\rho_a + \mu_a + \theta_{ac}) - \frac{\epsilon_2^2}{2}\right] t + \mathcal{H}_2(t) \\ &= \ln I_a(0) + \left[\beta_a(1-\kappa\zeta) - (\rho_a + \mu_a + \theta_{ac}) - \frac{\epsilon_2^2}{2}\right] t + \mathcal{H}_2(t),\end{aligned} \tag{33}$$

where $\mathcal{H}_2(t) = \int_0^t \epsilon_2 dB_2(t)$ is a martingale .

Next, we divide through (33) by t, find $\limsup_{t\to\infty}$ and use Lemma (1) to get

$$\begin{aligned}\limsup_{t\to\infty} \frac{\ln I_a(t)}{t} &= \limsup_{t\to\infty} \frac{\ln I_a(0)}{t} + \left[\lambda_a S(t) - (\rho_a + \mu_a + \theta_{ac}) - \frac{\epsilon_2^2}{2}\right] t \\ &\quad + \limsup_{t\to\infty} \frac{\mathcal{H}_2(t)}{t} \\ &= \left[\beta_a(1-\kappa\zeta) - (\rho_a + \mu_a + \theta_{ac}) - \frac{\epsilon_2^2}{2}\right] \\ &= (\rho_a + \mu_a + \theta_{ac}) \left[\frac{\beta_a(1-\kappa\zeta)}{(\rho_a + \mu_a + \theta_{ac})} - 1 - \frac{\epsilon_2^2}{2(\rho_a + \mu_a + \theta_{ac})}\right] \\ &= (\rho_a + \mu_a + \theta_{ac}) \left(\mathcal{R}_{0a}^s - 1\right).\end{aligned}$$

For

$$\limsup_{t\to\infty} \frac{\ln I_a(t)}{t} = (\rho_a + \mu_a + \theta_{ac}) \left(\mathcal{R}_{0a}^s - 1\right) < 0,$$

$$\mathcal{R}_{0a}^s - 1 < 0,$$

since

$$(\rho_a + \mu_a + \theta_{ac}) > 0.$$

This implies that whenever $\mathcal{R}_{0a}^s < 1$, $\limsup_{t\to\infty} \dfrac{\ln I_a(t)}{t} \leq 0.$ □

3.5.5 Global Stability of HBV Only Model

Theorem 8. *If $\mathcal{R}_{0a}^s < 1$, then E_{0a} is globally asymptotically stable in Ω.*

Proof. We consider a Lyapunov function L_2 , see, e.g., [45],

$$L_2(t) = \left[\psi + \alpha\delta + \frac{\psi\theta}{\mu\delta}\right] I_a(t).$$

We differentiate to obtain

$$\frac{dL_2}{dt} = \left[\psi + \alpha\delta + \frac{\psi\theta}{\mu\delta}\right] \frac{dI_a(t)}{dt}. \tag{34}$$

We substitute $dI_a(t)$, into (34), and then solving at DFE we get

$$\begin{aligned}\frac{dL_2}{dt} &= \left[\psi + \alpha\delta + \frac{\psi\theta}{\mu\delta}\right] \big(\lambda_a S(t) - (\theta_{ac} + \rho_a + \mu_a) + \epsilon_2 dB_2(t)\big) I_a(t) \\ &= \left[\psi + \alpha\delta + \frac{\psi\theta}{\mu\delta}\right] (\rho_a + \mu_a + \theta_{ac}) \Big[\frac{\beta_a(1-\kappa\zeta)}{(\rho_a + \mu_a + \theta_{ac})} - 1 - \frac{\epsilon_2 dB_2(t)}{(\rho_a + \mu_a + \theta_{ac})}\Big] I_a(t).\end{aligned}$$

Clearly

$$\left[\psi + \alpha\delta + \frac{\psi\theta}{\mu\delta}\right](\rho_a + \mu_a + \theta_{ac}) > 0.$$

For

$$\frac{dL_2}{dt} < 0,$$

$$\Big[\frac{\beta_a(1-\kappa\zeta)}{(\rho_a+\mu_a+\theta_{ac})} - 1 + \frac{\epsilon_2 dB_2(t)}{(\rho_a+\mu_a+\theta_{ac})}\Big] < 0.$$

By comparison we obtain

$$\begin{aligned}\Big[\frac{\beta_a(1-\kappa\zeta)}{(\rho_a+\mu_a+\theta_{ac})} - 1 - \frac{\epsilon_2^2}{2(\rho_a+\mu_a+\theta_{ac})}\Big] \quad &< \\ \Big[\frac{\beta_a(1-\kappa\zeta)}{(\rho_a+\mu_a+\theta_{ac})} - 1 + \frac{\epsilon_2 dB_2(t)}{(\rho_a+\mu_a+\theta_{ac})}\Big] &< 0.\end{aligned}$$

From (30) we conclude

$$\begin{aligned}\mathcal{R}^s_{0a} - 1 &< 0 \\ \mathcal{R}^s_{0a} &< 1.\end{aligned}$$

Hence L_2 is globally stable in the domain Ω. □

3.6 Reproductive Number of Co-infection Model

In this section we present results on the Reproductive Number for the deterministic co-infection model, $\mathcal{R}^d_{0aC}$, and the reproductive number for the co-infection model in the stochastic sense $\mathcal{R}^s_{0aC}$. Next we determine stability conditions for $\mathcal{R}^d_{0aC}$, and $\mathcal{R}^s_{0aC}$ respectively.

3.6.1 Reproductive Number of Deterministic Co-infection Model

In this section, we employ the next generation matrix [9] method to determine the basic reproductive number of the deterministic co-infection model. As explained earlier, the NGM method for determining the basic reproductive number requires that we first find f, the matrix of new infections and v, the matrix of secondary infections respectively. We therefore proceed by considering only disease infectious states of (2) we have

$$\begin{cases} \dfrac{dS(t)}{dt} & = \psi + \sigma_V V_C(t) + \sigma_{aC} R_{aC}(t) + \sigma_C R_C(t) - (\lambda_a I_a(t) + \lambda_C I_C(t))S(t) \\ & \quad -(\mu + \theta_V)S(t) \\ \dfrac{dI_a(t)}{dt} & = \lambda_a I_a(t)S(t) - (\theta_{ac} + \rho_a + \eta_C + \mu_a)I_a(t) \\ \dfrac{dI_C(t)}{dt} & = \lambda_C I_C(t)S(t) - (\eta_a + \rho_C + \mu_C)I_C(t) \\ \dfrac{dI_{aC}(t)}{dt} & = (\eta_C I_a(t) + \eta_a I_C(t)) - (\rho_{aC} + \theta_{acC} + \mu_{aC})I_{aC}(t) \end{cases} \tag{35}$$

with initial conditions $S(0) > 0$, $I_C(0) \geq 0$, $I_a(0) \geq 0$, $I_{aC}(0) \geq 0$, $I_c(0) \geq 0$, $I_{cC}(0) \geq 0$. $\lambda_a I_a S$ and $\lambda_C I_C S$ represent new infections.$\eta_C I_a I_{aC}$ and $\eta_a I_C I_{aC}$ represent progression to co-infection. We determine f which represents primary or new infections from the susceptible compartment and v

which represents the rate of transition from one compartment to the other. These are represented as

$$f = \begin{pmatrix} \lambda_a I_a(t)S(t) \\ \lambda_C I_C(t)S(t) \\ \eta_C I_a I_{aC} + \eta_a I_C I_{aC} \end{pmatrix} \tag{36}$$

and

$$v = \begin{pmatrix} (\theta_{ac} + \rho_a + \eta_C I_{aC} + \mu_a)I_a(t) \\ (\eta_a I_{aC} + \rho_C + \mu_C)I_C(t) \\ (\rho_{aC} + \theta_{acC} + \mu_{aC})I_{aC}(t) \end{pmatrix}. \tag{37}$$

Using the NGM method we seek to determine the basic reproductive number which is the spectra radius of the FV^{-1}. Finding the partial derivatives F and V and evaluating at DFE gives,

$$F = \begin{pmatrix} \lambda_a S & 0 & 0 \\ 0 & \lambda_C S & 0 \\ \eta_C I_a & \eta_a I_C & 0 \end{pmatrix} \tag{38}$$

$$V = \begin{pmatrix} \theta_{ac} + \rho_a + \eta_C I_{aC} + \mu_a & 0 & 0 \\ 0 & \eta_a I_{aC} + \rho_C + \mu_C & 0 \\ 0 & 0 & \rho_{aC} + \theta_{acC} + \mu_{aC} \end{pmatrix} \tag{39}$$

Next, we determine FV^{-1}, where $V^{-1} = \frac{1}{detV}(adjV)$. V^{-1} is computed as

$$V^{-1} = \begin{pmatrix} \dfrac{1}{\theta_{ac} + \rho_a + \eta_C I_{aC} + \mu_a} & 0 & 0 \\ 0 & \dfrac{1}{\eta_a I_{aC} + \rho_C + \mu_C} & 0 \\ 0 & 0 & \dfrac{1}{\rho_{aC} + \theta_{acC} + \mu_{aC}} \end{pmatrix} \tag{40}$$

Multiplying F and V^{-1} gives

$$FV^{-1} = \begin{pmatrix} \dfrac{\lambda_a S}{\theta_{ac} + \rho_a + \eta_C I_{aC} + \mu_a} & 0 & 0 \\ 0 & \dfrac{\lambda_C S}{\eta_a I_{aC} + \rho_C + \mu_C} & 0 \\ \dfrac{\eta_C I_a}{\rho_{aC} + \theta_{acC} + \mu_{aC}} & \dfrac{\eta_a I_C}{\rho_{aC} + \theta_{acC} + \mu_{aC}} & 0 \end{pmatrix} \tag{41}$$

$$FV^{-1}|_{DFE} = \begin{pmatrix} \frac{\beta_a(1-\delta\zeta)}{\theta_{ac}+\rho_a+\mu_a} & 0 & 0 \\ 0 & \frac{\beta_a(1-\kappa\zeta)}{\rho_C+\mu_C} & 0 \\ 0 & 0 & 0 \end{pmatrix} \tag{42}$$

where

$$\mathcal{R}^d_{0a} = \frac{\beta_a(1-\delta\zeta)}{\theta_{ac} + \rho_a + \mu_a}, \text{ and } \mathcal{R}^d_{0C} = \frac{\beta_C(1-\kappa\zeta)}{\eta_a + \rho_C + \mu_c}$$

are basic reproduction numbers for the deterministic HBV and COVID-19 only models in the co-infection model (2).

The basic reproduction numbers $\mathcal{R}^d_{0ac}$ associated with (2) is given by the spectral radius (i.e. largest eigenvalue) of FV^{-1}. Hence, reproduction number for the full model system (2) is given by

$$\mathcal{R}^d_{0aC} = \max(\mathcal{R}_{0a}, \mathcal{R}_{0C}).$$

3.6.2 Basic Reproductive Number of Stochastic Co-infection Model

In this section we determine the reproduction number of the COVID-19 and acute HBV stochastic co-infection model. We consider the co-infected class of (3).

$$\begin{aligned}\frac{dI_{aC}(t)}{dt} &= (\eta_C I_a(t) + \eta_a I_C(t))I_{aC}(t) - (\rho_{aC} + \theta_{acC} + \mu_{aC})I_{aC})(t) \\ &\quad + \epsilon_4 I_{aC} dB_4(t) + \int_{\mathcal{U}} \Psi_3(u) I_{aC}(s^-)\tilde{\mathcal{N}}(dt, du).\end{aligned} \tag{43}$$

We set a function $g(t, I_C(t)) = \ln(t, I_C(t))$. Applying Itô- Lévy formula to (43), we obtain

$$\begin{aligned}d\ln I_{aC}(t) = &\Big[(\eta_C I_a(t) + \eta_a I_C(t)) - (\rho_{aC} + \theta_{acC} + \mu_{aC}) - \frac{\epsilon_4^2}{2} \\ &+ \int_{\mathcal{U}} (\Psi_3(u) - \ln(1 + \Psi_3(u)))v(du)\Big]dt + \epsilon_4 dB_4(t) \\ &+ \int_{\mathcal{U}} \ln(1 + \Psi_3(u))\tilde{\mathcal{N}}(dt, du).\end{aligned} \tag{44}$$

Considering partial derivatives with respect to I_{aC} of the initial infections F and of secondary infections V, we determine the basic reproduction number by means of the next generation matrix [9] as follows

$$\begin{aligned}F &= \eta_C I_a + \eta_a I_C - \frac{1}{2}\epsilon_4^2 - \int_{\mathcal{U}} (\Psi_3(u) - \ln(1 + \Psi_3(u)))v(du) \\ &= \frac{\beta_C(1 - \kappa\zeta)I_a}{N} + \frac{\beta_a(1 - \kappa\zeta)I_C}{N} - \frac{1}{2}\epsilon_4^2 - \int_{\mathcal{U}} (\Psi_3(u) - \ln(1 + \Psi_3(u)))v(du).\end{aligned}$$

Since

$$I_C, I_a < N \leq \frac{\psi}{\mu},$$

we have

$$F \leq \beta_C(1 - \kappa\zeta) + \beta_C(1 - \delta\zeta) - \frac{1}{2}\epsilon_4^2 - \int_{\mathcal{U}} (\Psi_3(u) - \ln(1 + \Psi_3(u)))v(du).$$

Also

$$V = (\rho_{aC} + \theta_{acC} + \mu_{aC}).$$

Multiplying F and V^{-1} and factorising $(\rho_{aC} + \theta_{acC} + \mu_{aC})$ we get

$$\begin{aligned}FV^{-1} \leq (\rho_{aC} + \theta_{acC} + \mu_{aC})^{-1}\Big[&\beta_C(1 - \kappa\zeta) + \beta_C(1 - \delta\zeta) - \frac{1}{2}\epsilon_4^2 \\ &- \int_{\mathcal{U}} (\Psi_3(u) - \ln(1 + \Psi_3(u)))v(du)\Big].\end{aligned}$$

Taking the spectral radius of FV^{-1}, i.e. $\rho(FV^{-1}) = \mathcal{R}^s_{0aC}$, we obtain

$$\begin{aligned}\mathcal{R}^s_{0aC} = (\rho_{aC} + \theta_{acC} + \mu_{aC})^{-1}\Big(&\beta_C(1 - \kappa\zeta) + \beta_C(1 - \delta\zeta) - \frac{1}{2}\epsilon_4^2 \\ &- \int_{\mathcal{U}} (\Psi_3(u) - \ln(1 + \Psi_3(u)))v(du)\Big).\end{aligned} \tag{45}$$

3.6.3 Local Stability of Deterministic Co-infection Model

Theorem 9. *The Co-infection disease free equilibrium point is locally asymptotically stable if and only if $\mathcal{R}^d_{0aC} < 1$ and unstable otherwise.*

Proof. We recall (10). The local stability of the COVID-19-HBV co-infection disease free equilibrium is established by showing that the eigenvalues of Jacobian of the system, $J(Q)$, are all negative and the determinant at DFE, $\det(J(E_0)) > 0$. First, we derived the Jacobian matrix of model (2) as

$$J = \begin{pmatrix} M_1 & -\lambda_a S & -\lambda_C S & 0 & 0 & 0 & 0 & 0 & 0 & 0 & 0 & 0 & \theta_V \\ \lambda_a I_a & M_2 & 0 & -\eta_C I_a & 0 & 0 & 0 & 0 & 0 & 0 & 0 & 0 & 0 \\ \lambda_C I_C & 0 & M_3 & -\eta_a I_C & 0 & 0 & 0 & 0 & 0 & 0 & 0 & 0 & 0 \\ 0 & \eta_C I_a & \eta_a I_C & M_4 & 0 & 0 & 0 & 0 & 0 & 0 & 0 & 0 & 0 \\ 0 & \theta_{ac} & 0 & 0 & M_5 & 0 & 0 & 0 & 0 & 0 & 0 & 0 & 0 \\ 0 & 0 & 0 & \theta_{acC} & \sigma_c & M_6 & 0 & 0 & 0 & 0 & 0 & 0 & 0 \\ 0 & \rho_a & 0 & 0 & 0 & 0 & M_7 & 0 & 0 & 0 & 0 & 0 & 0 \\ 0 & 0 & \rho_{aC} & 0 & 0 & 0 & 0 & M_8 & 0 & 0 & 0 & 0 & 0 \\ 0 & 0 & \rho_C & \rho_{cC} & 0 & 0 & 0 & 0 & M_9 & 0 & 0 & 0 & 0 \\ 0 & 0 & 0 & 0 & 0 & 0 & \phi_a & 0 & 0 & M_{10} & 0 & 0 & 0 \\ 0 & 0 & 0 & 0 & 0 & 0 & 0 & \phi_{aC} & 0 & 0 & M_{11} & 0 & 0 \\ 0 & 0 & 0 & 0 & 0 & 0 & 0 & 0 & \phi_C & 0 & 0 & M_{12} & 0 \\ 0 & 0 & 0 & 0 & 0 & 0 & 0 & 0 & 0 & 0 & 0 & 0 & M_{13} \end{pmatrix}$$

where $M_1 = -\lambda_a I_a - \lambda_C I_C - (\mu + \theta_V)$, $M_2 = -(\theta_{ac} + \rho_a + \eta_C I_{aC} + \mu_a)$, $M_3 = -(\eta_a I_{aC} + \rho_C + \mu_C)$, $M_4 = -(\rho_{aC} + \theta_{acC} + \mu_{aC})$, $M_5 = -(\sigma_c + \mu_c)$, $M_6 = -(\mu_{cC} + \rho_{cC})$, $M_7 = -(\mu + \phi_a)$, $M_8 = -(\mu + \phi_{aC})$, $M_9 = -(\mu + \phi_C + \phi_{cC})$, $M_{10} = -\mu$, $M_{11} = -(\mu + \sigma_{aC})$, $M_{12} = -(\mu + \sigma_C)$, $M_{13} = -(\mu + \sigma_V)$. Next, we solve J at the disease free equilibrium point and obtain $J(E_0)$. Then determine the characteristic matrix by $\det(J(E_{0C}) - \lambda I)$, where I is the identity matrix. The corresponding characteristic equation is given as

$$\begin{aligned} y = {} & ((-\beta_a(1-\delta\zeta) - \beta_C(1-\kappa\zeta) - (\mu+\theta_V)) - \lambda)((-\theta_{ac} - \rho_a - \mu_a) - \lambda) \\ & ((-\rho_C - \mu_C) - \lambda)((-\rho_{aC} - \theta_{acC} - \mu_{aC}) - \lambda)((-\sigma_c - \mu_c) - \lambda) \\ & ((-\mu_{cC} - \rho_{cC}) - \lambda)((-\mu - \phi_a) - \lambda)((-\mu - \phi_{aC} - \lambda)) \\ & ((-\mu - \phi_C - \phi_{cC}) - \lambda)((-\mu) - \lambda)((-\mu - \sigma_{aC}) - \lambda)((-\mu - \sigma_C) - \lambda) \\ & ((-\mu - \sigma_V) - \lambda). \end{aligned}$$

By letting $\det(J(E_0) - \lambda I) = 0$, we observe that the thirteen eigenvalues are negative, since all parameters are non-negative. Also, since the Jacobian matrix at DFE is lower triangular, its determinant is obtained as the product of its diagonal elements as follows

$$\det(J(E_0)) = M_1 M_2 M_3 M_4 M_5 M_6 M_7 M_8 M_9 M_{10} M_{11} M_{12} M_{13}$$

where $M_2, M_3, \ldots, M_{13}$ are strictly negative because they represent death rates, recovery rates, and transition rates, which are always positive. The determinant remains positive if $M_1 > 0$, hence

$$\beta_C(1-\kappa\zeta) + \beta_a(1-\delta\zeta) + (\mu + \theta_V) < 0.$$

For $(\rho_{aC} + \theta_{acC} + \mu_{aC}) < (\mu + \theta_V)$ we conclude that the DFE is locally stable when

$$\mathcal{R}^d_{0aC} = \frac{\beta_a(1-\delta\zeta)}{(\rho_{aC} + \theta_{acC} + \mu_{aC})} + \frac{\beta_C(1-\delta\zeta)}{(\rho_{aC} + \theta_{acC} + \mu_{aC})} < 1.$$

□

3.6.4 Local Stability of Disease Free Equilibrium point in the Co-infection Model

Theorem 10. *If $\mathcal{R}^s_{0aC} < 1$, then for any initial values of $(S(0), I_C(0), I_a(0), I_{aC}(0), I_c(0), I_{cC}(0), T_a(0), T_C(0), T_{aC}(0), R_a(0), R_C(0), R_{aC}(0), V_C(0)) \in \Re^{13}$, $I_{aC}(t)$ satisfies $\limsup_{t\to\infty} \frac{\ln I_{aC}(t)}{t} \leq 0$.*

Proof. We set a function $g(t, I_{aC}(t)) = \ln(t, I_{aC}(t))$, and apply Itô- Lévy formula to the co-infected equation of (3) to obtain

$$\begin{aligned} d\ln I_{aC}(t) = &\left[(\eta_C I_a(t) + \eta_a I_C(t)) - (\rho_{aC} + \theta_{acC} + \mu_{aC}) - \frac{\epsilon_4^2}{2} + \int_{\mathcal{U}} (\Psi_3(u) - \ln(1+\Psi_3(u)))v(du)\right]dt \\ &+ \epsilon_4 dB_4(t) + \int_{\mathcal{U}} \ln(1+\Psi_3(u))\tilde{\mathcal{N}}(dt, du). \end{aligned} \tag{46}$$

Next, we integrate both sides (46) to get

$$\begin{aligned} \ln I_{aC}(t) = &\eta_C \int_0^t I_a(r)dr + \eta_a \int_0^t I_C(r)dr - (\rho_{aC} + \theta_{acC} + \mu_{aC})t - \frac{\epsilon_4^2}{2}t + \epsilon_4 \int_0^t dB_4(t) \\ &+ \int_0^t \int_{\mathcal{U}} \ln(1+\Psi_3(u))\tilde{\mathcal{N}}(dt, du) + \ln I_{aC}(0). \end{aligned} \tag{47}$$

Evaluating at DFE, and since

$$I_C, I_a < N \leq \frac{\psi}{\mu},$$

we have

$$\begin{aligned} \ln I_{aC}(t) \leq &\frac{\beta_C(1-\kappa\zeta)}{N} \int_0^t \frac{\psi}{\mu} dr + \frac{\beta_a(1-\delta\zeta)}{N} \int_0^t \frac{\psi}{\mu} dr - (\rho_{aC} + \theta_{acC} + \mu_{aC})t \\ &- \frac{\epsilon_4^2}{2}t + \epsilon_4 \int_0^t dB_4(t) + \int_0^t \int_{\mathcal{U}} \ln(1+\Psi_3(u))\tilde{\mathcal{N}}(dt, du) + \ln I_{aC}(0) \\ \leq &\frac{\beta_C(1-\kappa\zeta)}{N} \frac{\psi}{\mu} t + \frac{\beta_a(1-\delta\zeta)}{N} \frac{\psi}{\mu} t - (\rho_{aC} + \theta_{acC} + \mu_{aC})t - \frac{\epsilon_4^2}{2}t \\ &+ \epsilon_4 \int_0^t dB_4(t) + \int_0^t \int_{\mathcal{U}} \ln(1+\Psi_3(u))\tilde{\mathcal{N}}(dt, du) + \ln I_{aC}(0) \\ \leq &\beta_C(1-\kappa\zeta)t + \beta_a(1-\delta\zeta)t - (\rho_{aC} + \theta_{acC} + \mu_{aC})t - \frac{\epsilon_4^2}{2}t \\ &+ \epsilon_4 \int_0^t dB_4(t) + \int_0^t \int_{\mathcal{U}} \ln(1+\Psi_3(u))\tilde{\mathcal{N}}(dt, du) + \ln I_{aC}(0). \end{aligned} \tag{48}$$

We let $\mathbf{G} = (\rho_{aC} + \theta_{acC} + \mu_{aC})$, $\mathcal{E}_3 = \int_{\mathcal{U}} (\Psi_3(u) - \ln(1 + \Psi_4(u)))v(du)$, $\mathcal{H}_3(t) = \int_0^t \epsilon_4 dB_4(t)$, and $\mathcal{A}_3 = \int_0^t \int_{\mathcal{U}} \ln(1 + \Psi_3(u))\tilde{\mathcal{N}}(ds, du)$. Next, we divide through (48) by t, find $\limsup_{t\to\infty}$ and apply Lemma (1) as follows,

$$\begin{aligned}
\limsup_{t\to\infty} \frac{\ln I_{aC}(t)}{t} &\leq \limsup_{t\to\infty} \frac{\ln I_{aC}(0)}{t} + \Big[\beta_C(1-\kappa\zeta)t + \beta_a(1-\delta\zeta)t \\
&\quad - \mathbf{G} - \frac{\epsilon_4^2}{2} - \mathcal{E}_3\Big] + \limsup_{t\to\infty} \frac{\mathcal{H}_3(t)}{t} + \limsup_{t\to\infty} \frac{\mathcal{A}_3}{t} \\
&\leq (\rho_{aC} + \theta_{acC} + \mu_{aC})\Big[\frac{\beta_a(1-\kappa\zeta)}{\mathbf{G}} + \frac{\beta_c(1-\kappa\zeta)}{\mathbf{G}} \\
&\quad - 1 - \frac{\epsilon_4^2}{2\mathbf{G}} - \frac{\mathcal{E}_3}{\mathbf{G}}\Big].
\end{aligned}$$

From (45) we have

$$\limsup_{t\to\infty} \frac{\ln I_{aC}(t)}{t} \leq (\rho_{aC} + \theta_{acC} + \mu_{aC})\,(\mathcal{R}^s_{0aC} - 1) < 0.$$

Clearly

$$\rho_{aC} + \theta_{acC} + \mu_{aC} > 0.$$

If

$$\limsup_{t\to\infty} \frac{\ln I_{aC}(t)}{t} \leq 0.$$

then

$$\mathcal{R}^s_{0aC} - 1 < 0.$$

We conclude that whenever $\mathcal{R}^s_{0aC} < 1$, $\limsup_{t\to\infty} \dfrac{\ln I_{aC}(t)}{t} \leq 0$. □

3.6.5 Global Stability of Co-infection Model

Theorem 11. *If $\mathcal{R}^s_{0aC} < 1$, then E_{0aC} is globally asymptotically stable in Ω.*

Proof. We consider a Lyapunov function L_3 , see, e.g., [45],

$$L_3(t) = \left[\psi + \alpha\delta + \frac{\psi\theta}{\mu\delta}\right] I_{aC}(t), \tag{49}$$

Differentiating (49) and substitution yields

$$\begin{aligned}
\frac{dL_3(t)}{dt} &= \left[\psi + \alpha\delta + \frac{\psi\theta}{\mu\delta}\right] \frac{dI_{aC}(t)}{dt} \\
&= \left[\psi + \alpha\delta + \frac{\psi\theta}{\mu\delta}\right]\Big[(\eta_C I_a(t) + \eta_a I_C(t)) - (\rho_{aC} + \theta_{acC} + \mu_{aC}) \\
&\quad + \epsilon_4 dB_4(t) + \int_{\mathcal{U}} \Psi_2(u) I_{aC}(s^-)\tilde{\mathcal{N}}(dt, du)\Big] I_{aC}(t).
\end{aligned} \tag{50}$$

Solving (50) at DFE, and since $0 \leq I_a(t), I_C(t) \leq N(t) \leq \frac{\psi}{\mu}$ we obtain

$$\frac{dL_3(t)}{dt} = \left[\psi + \alpha\delta + \frac{\psi\theta}{\mu\delta}\right](\rho_{aC} + \theta_{acC} + \mu_{aC})\left[\frac{\beta_C(1-\kappa\zeta)}{\mathbf{G}} + \frac{\beta_a(1-\delta\zeta)}{\mathbf{G}} - 1 + \frac{\epsilon_4}{\mathbf{G}} - \frac{\mathbb{B}_3}{\mathbf{G}}\right] I_{aC}(t),$$

where $\mathbb{B}_3 = \int_{\mathcal{U}} \Psi_4(u)\tilde{\mathcal{N}}(dt, du), \mathbf{G} = (\rho_{aC} + \theta_{acC} + \mu_{aC})$, and $\mathcal{E}_3 = \int_{\mathcal{U}}(\Psi_4(u) - \ln(1 + \Psi_4(u)))v(du)$. Clearly

$$\left[\psi + \alpha\delta + \frac{\psi\theta}{\mu\delta}\right](\rho_{aC} + \theta_{acC} + \mu_{aC}) > 0.$$

For

$$\frac{dL_3}{dt} < 0,$$

$$\left[\frac{\beta_a(1-\delta\zeta)}{\mathbf{G}} + \frac{\beta_C(1-\kappa\zeta)}{\mathbf{G}} - 1 + \frac{\epsilon_4}{\mathbf{G}} - \frac{\mathbb{B}_3}{\mathbf{G}}\right] < 0.$$

By comparison we obtain

$$\left[\frac{\beta_a(1-\delta\zeta)}{\mathbf{G}} + \frac{\beta_C(1-\kappa\zeta)}{\mathbf{G}} - 1 - \frac{\epsilon_4}{2\mathbf{G}} - \frac{\mathbb{B}_3}{\mathbf{G}}\right] <$$
$$\left[\frac{\beta_a(1-\delta\zeta)}{\mathbf{G}} + \frac{\beta_C(1-\kappa\zeta)}{\mathbf{G}} - 1 + \frac{\epsilon_4^2}{\mathbf{G}} - \frac{\mathbb{B}_3}{\mathbf{G}}\right] < 0.$$

From (45) we conclude

$$\mathcal{R}^s_{0aC} - 1 < 0$$
$$\mathcal{R}^s_{0aC} < 1.$$

Hence L_3 is globally stable in the domain Ω. □

3.7 Extinction of HBV- COVID-19 co-infection Disease

Next, we determine conditions under which the disease will eventually die out in the population with a probability of one. In this section, we study the conditions of extinction for the co-infection model.

Definition 3 ([1]). *We define* $\langle I_a(t)\rangle = \frac{1}{t}\int_0^t I_a(r)dr$, *and* $\langle I_C(t)\rangle = \frac{1}{t}\int_0^t I_C(r)dr$.

Lemma 1 ([67]). *Let* $(S(t), I_C(t), I_a(t), I_{aC}(t), I_c(t), I_{cC}(t), T_a(t), T_C(t), T_{aC}(t), R_a(t), R_C(t), R_{aC}(t), V_C(t))$ *be the positive solution of system* (4) *with given initial condition* $(S(0), I_C(0), I_a(0), I_{aC}(0), I_c(0), I_{cC}(0), T_a(0), T_C(0), T_{aC}(0), R_a(0), R_C(0), R_{aC}(0), V_C(0)) \in \Re^{13}_+$. *Let also N(t) be the positive solution of equation* (4) *with given initial condition given condition* $N(0) = S(0) + I_C(0) + I_a(0) + I_{aC}(0) + I_c(0) + I_{cC}(0) + T_a(0) + T_C(0) + T_{aC}(0) + R_a(0) + R_C(0) + R_{aC}(0) + V_C(0) \in \Re_+$. *Then*

1. $\lim_{t\to\infty} \frac{N(t)}{t} = 0$
2. $\limsup_{t\to\infty} \frac{N(t)}{t} = 0$
3. $\lim_{t\to\infty} \frac{1}{t}\int_0^t N(s)dW(s) = 0$, *and*

4. $\lim_{t\to\infty}\frac{1}{t}\int_0^t\int_{\mathcal{U}}\eta(u)N(t^-)\tilde{\mathcal{N}}=0,$ *a.s.*

Theorem 12. *Let* $(S(t), I_C(t), I_a(t), I_{aC}(t), I_c(t), I_{cC}(t), T_a(t), T_C(t), T_{aC}(t), R_a(t), R_C(t), R_{aC}(t), V_C(t))$ *be the solution of* (3) *with initial values* $\big(S(0), I_C(0), I_a(0), I_{aC}(0), I_c(0), I_{cC}(0), T_a(0), T_C(0), T_{aC}(0), R_a(0), R_C(0), R_{aC}(0), V_C(0)\in\Omega\big)$, *the co-infection disease of model* (3) *goes extinct almost surely* $(\lim_{t\to\infty} I_{aC}(t)=0)$ *if* $\mathcal{R}^s_{0aC}<1$.

Proof. Let $V_1=\ln I_{aC}(t)$ be the Lyapunov function, then the Itô- Lévy expression of the co-infected equation of (3)

$$\begin{aligned} d\ln I_{aC}(t) = &\Big[(\eta_C I_a(t)+\eta_a I_C(t)) - (\rho_{aC}+\theta_{acC}+\mu_{aC}) - \frac{\epsilon_4^2}{2} \\ &+ \int_{\mathcal{U}}(\Psi_2(u)-\ln(1+\Psi_2(u)))v(du)\Big]dt + \epsilon_4 dB_4(t) \\ &+ \int_0^t\int_{\mathcal{U}}\ln(1+\Psi_3(u))\tilde{\mathcal{N}}(ds,du). \end{aligned} \tag{51}$$

Next, we integrate both sides of (51) we obtain

$$\begin{aligned} \int_0^t d\ln I_{aC}(S) &= \eta_C\int_0^t I_a(r)dr + \eta_a\int_0^t I_C(r))dr - \int_0^t\big[(\rho_{aC}+\theta_{acC}+\mu_{aC})\big]dt \\ &\quad - \int_0^t\frac{\epsilon_4^2}{2}dr - \mathcal{E}_3 t + \mathcal{H}_3(t) + \mathcal{A}_3 \\ \ln I_{aC}(t) &= \eta_C\int_0^t I_a(r)dr + \eta_a\int_0^t I_C(r))dr - \big[(\rho_{aC}+\theta_{acC}+\mu_{aC})\big]t \\ &\quad - \frac{\epsilon_4^2}{2}t - \mathcal{E}_3 t + \mathcal{H}_3(t) + \mathcal{A}_3 + \ln I_{aC}(0), \end{aligned}$$

where $\mathcal{E}_3=\int_{\mathcal{U}}(\Psi_3(u)-\ln(1+\Psi_3(u)))v(du)$, $\mathcal{H}_3(t)=\int_0^t\epsilon_4 dB_4(t)$, and $\mathcal{A}_3=\int_0^t\int_{\mathcal{U}}\ln(1+\Psi_3(u))\tilde{\mathcal{N}}(ds,du)$.

Since $0\le I_C(t), I_a(t) < N(t) < \frac{\psi}{\mu}$, we choose a constant $C=\frac{\psi}{\mu}$, and let $I_C(t)=I_a(t)=C=\frac{\psi}{\mu}$ to get

$$\begin{aligned} \ln I_{aC}(t) &\le \eta_C\int_0^t\frac{\psi}{\mu}dr + \eta_a\int_0^t\frac{\psi}{\mu}dr - (\rho_{aC}+\theta_{acC}+\mu_{aC})t - \frac{\epsilon_4^2}{2}t \\ &\quad - \mathcal{E}_3 t + \mathcal{H}_3(t) + \mathcal{A}_3 + \ln I_{aC}(0) \\ &\le \eta_C\frac{\psi}{\mu}t + \eta_a\frac{\psi}{\mu}t - (\rho_{aC}+\theta_{acC}+\mu_{aC})t - \frac{\epsilon_4^2}{2}t - \mathcal{E}_3 t + \mathcal{H}_3(t) \\ &\quad + \mathcal{A}_3 + \ln I_{aC}(0). \end{aligned} \tag{52}$$

We divide through (52) by t to obtain

$$\begin{aligned} \frac{\ln I_{aC}(t)}{t} &\le \eta_C\frac{\psi t}{\mu t} + \eta_a\frac{\psi t}{\mu t} - \frac{(\rho_{aC}+\theta_{acC}+\mu_{aC})t}{t} - \frac{\epsilon_4^2 t}{2t} \\ &\quad - \frac{\mathcal{E}_3}{t} + \frac{\mathcal{H}_3(t)}{t} + \frac{\mathcal{A}_3}{t} + \frac{\ln I_{aC}(0)}{t} \\ &\le \beta_C(1-\kappa\zeta) + \beta_a(1-\delta\zeta) - \frac{(\rho_{aC}+\theta_{acC}+\mu_{aC})t}{t} \\ &\quad - \frac{\epsilon_4^2 t}{2t} - \frac{\mathcal{E}_3}{t} + \frac{\mathcal{H}_3(t)}{t} + \frac{\mathcal{A}_3}{t} + \frac{\ln I_{aC}(0)}{t}. \end{aligned} \tag{53}$$

Next, we find the $\limsup_{t\to\infty}$ on both sides, apply Lemma (1), and factorise to obtain

$$\begin{aligned}\limsup_{t\to\infty}\frac{\ln I_{aC}(t)}{t} &\leq \limsup_{t\to\infty}\Big[\beta_C(1-\kappa\zeta)+\beta_a(1-\delta\zeta)-(\rho_{aC}+\theta_{acC}+\mu_{aC})\\ &\quad -\frac{\epsilon_2^2}{2}t\Big]+\limsup_{t\to\infty}\mathcal{E}_3+\limsup_{t\to\infty}\frac{\mathcal{H}_3(t)}{t}+\limsup_{t\to\infty}\frac{\mathcal{A}_3}{t}\\ &\quad +\limsup_{t\to\infty}\frac{\ln I_{aC}(0)}{t}\\ &\leq \Big[\beta_C(1-\kappa\zeta)+\beta_a(1-\delta\zeta)-(\rho_{aC}+\theta_{acC}+\mu_{aC})\\ &\quad -\frac{\epsilon_2^2}{2}t\Big]+\mathcal{E}_3\\ &\leq (\rho_{aC}+\theta_{acC}+\mu_{aC})\Big[\frac{\beta_C(1-\kappa\zeta)}{\mathbf{G}}+\frac{\beta_a(1-\delta\zeta)}{\mathbf{G}}\\ &\quad -1-\frac{\epsilon_2^2}{2\mathbf{G}}+\frac{\mathcal{E}_3}{\mathbf{G}}\Big],\end{aligned}$$

where $\mathbf{G}=(\rho_{aC}+\theta_{acC}+\mu_{aC})$. From (45) we have

$$\limsup_{t\to\infty}\frac{\ln I_{aC}(t)}{t}\leq(\rho_{aC}+\theta_{acC}+\mu_{aC})\Big(\mathcal{R}^s_{0aC}-1\Big).$$

Clearly $\mathbf{G}=(\rho_{aC}+\theta_{acC}+\mu_{aC})>0$.
If

$$\lim_{t\to\infty}\sup\frac{\ln I_{aC}(t)}{t}\leq 0.$$

then

$$(\mathcal{R}^s_{0aC}-1)<0.$$

From (1) we conclude that whenever $(\mathcal{R}^s_{0aC}-1)\leq 0$,

$$\limsup_{t\to\infty}\frac{\ln I_{aC}(t)}{t}\leq 0 \text{ which implies } \lim_{t\to\infty}I_{aC}(t)=0.$$

□

Next we determine the condition for extinction of HBV only disease in the population.

Theorem 13. *Let $(S(t),I_a(t),I_c(t),T_a(t),R_a(t))$ be the solution of HBV only model from* (3) *with initial values $\big(S(t),I_a(0),I_c(0),T_a(0),$
$R_a(0)\big)\in\Omega$, the HBV disease goes extinct almost surely* $(\lim_{t\to\infty}I_a(t)=0)$ *if $\mathcal{R}^s_{0H}<1$.*

Proof. Let $V_2=\ln I_a(t)$ be the Lyapunov function , then by applying Itô's formula we recall (18), which is the Itô expression for the HBV only infected class of (3)

$$d\ln I_a(t)=\Big[\lambda_aS(t)-(\theta_{ac}I_c(t)+\rho_a+\mu_a)-\frac{\epsilon_2^2}{2}\Big]dt+\epsilon_2dB_2(t).$$

We integrate both sides to get,

$$\begin{aligned}\int_0^t\ln I_a(r)&=\int_0^t\lambda_aS(r)dr-\int_0^t(\theta_{ac}+\rho_a+\mu_a)dr-\int_0^t\frac{\epsilon_2^2}{2}dr\\ &\quad+\epsilon_2\int_0^t dB_2(t).\end{aligned}$$

We know that $0 \leq S(t) < N(t) < \frac{\psi}{\mu}$, hence, we have

$$\ln I_a(t) - \ln I_a(0) \leq \beta_a(1-\delta\zeta) - (\theta_{ac} + \rho_a + \mu_a)t - \frac{\epsilon_2^2}{2}t + \int_0^t \epsilon_2 dB_2(r).$$

We divide through by t, find the $\limsup_{t\to\infty}$ on both sides, apply Lemma (1), and factorise to obtain

$$\begin{aligned}\limsup_{t\to\infty} \frac{\ln I_a(t)}{t} &\leq \limsup_{t\to\infty} \frac{\ln I_a(0)}{t} + \limsup_{t\to\infty} \frac{1}{t}\Big[\beta_a(1-\delta\zeta)t - (\theta_{ac} \\ &\quad + \rho_a + \mu_a)t - \frac{\epsilon_2^2}{2}t\Big] + \limsup_{t\to\infty} \frac{\mathcal{H}_1(t)}{t} \\ &= (\theta_{ac} + \rho_a + \mu_a)\Big[\frac{\beta_a(1-\delta\zeta)}{(\theta_{ac} + \rho_a + \mu_a)} - 1 \\ &\quad - \frac{\epsilon_2^2}{2(\theta_{ac} + \rho_a + \mu_a)}\Big],\end{aligned}$$

where $\mathcal{H}_1(t) = \int_0^t \epsilon_2 dB_2(t)$, is a martingale.
From (29) we have

$$\limsup_{t\to\infty} \frac{\ln I_a(t)}{t} \leq (\theta_{ac} + \rho_a + \mu_a)\left(\mathcal{R}_{0a}^s - 1\right).$$

Clearly,

$$(\theta_{ac} + \rho_a + \mu_a) > 0.$$

If

$$\lim_{t\to\infty} \sup \frac{\ln I_a(t)}{t} \leq 0,$$

then

$$\mathcal{R}_{0a}^s - 1 < 0,$$

From (1) we conclude that whenever $\mathcal{R}_{0a}^s \leq 1$,

$$\limsup_{t\to\infty} \frac{\ln I_a(t)}{t} \leq 0, \text{ and } \lim_{t\to\infty} I_a(t) = 0.$$

□

Next, we derive the condition for extinction of $I_C(t)$.

Theorem 14. *Let $(S(t), I_C(t), T_C(t), R_C(t), V_C(t))$ be the solution of COVID-19 only model from (3) with initial values $\big(S(0), I_C(0), T_C(0), R_C(0), V_C(0) \in \Omega\big)$, the COVID-19 disease goes extinct almost surely $(\lim_{t\to\infty} I_C(t) = 0)$ if $\mathcal{R}_{0C}^s < 1$.*

Proof. Let $V_3 = \ln I_C(t)$ be the Lyapunov function. Applying the Itô-Lévy formula gives

$$\begin{aligned}d\ln I_C(t) &= \Big[\lambda_C S(t) - (\rho_C + \mu_C) - \frac{\epsilon_3^2}{2} - \int_{\mathcal{U}} (\Psi_2(u) - \ln(1+\Psi_2(u)))v(du)\Big]dt \\ &\quad + \epsilon_3 dB_3(t) + \int_{\mathcal{U}} (\ln(1+\Psi_2(u))\tilde{\mathcal{N}}(dt, du),\end{aligned}$$

which is the Itô- Lévy expression for the COVID-19 infected class of the COVID only system of (3). Next, we integrate both sides to get,

$$\begin{aligned}\int_0^t \ln I_C(r) = \lambda_C \int_0^t S(r)dr - \int_0^t \Big(\rho_C + \mu_C + \frac{\epsilon_3^2}{2}\Big)dr + \int_0^t \epsilon_3 dB_3(r) \\ - \int_0^t \int_{\mathcal{U}} (\Psi_2(u) - \ln(1+\Psi_2(u)))v(du)dr \\ + \int_0^t \int_{\mathcal{U}} \ln(1+\Psi_2(u))\tilde{\mathcal{N}}(ds,du).\end{aligned}$$

We know that $0 \leq I_C(t) < N(t) < \frac{\psi}{\mu}$, hence,

$$\begin{aligned}\ln I_C(t) - \ln I_C(0) &\leq \lambda_C \int_0^t \frac{\psi}{\mu} dr - \Big(\rho_C + \mu_C + \frac{\epsilon_3^2}{2}\Big)t + \int_0^t \epsilon_3 dB_3(r) \\ &\quad - \int_0^t \int_{\mathcal{U}} (\Psi_2(u) \quad - \ln(1+\Psi_2(u)))v(du)dr \\ &\quad + \int_0^t \int_{\mathcal{U}} \ln(1+\Psi_2(u))\tilde{\mathcal{N}}(ds,du). \\ &\leq \beta_C(1-\kappa\zeta)t - \Big(\rho_C + \mu_c + \frac{\epsilon_3^2}{2}\Big)t + \int_0^t \epsilon_3 dB_3(r) \\ &\quad - \int_{\mathcal{U}} (\Psi_2(u) - \ln(1+\Psi_2(u)))v(du) \\ &\quad + t\int_0^t \int_{\mathcal{U}} \ln(1+\Psi_2(u))\tilde{\mathcal{N}}(ds,du).\end{aligned}$$

We divide through by t, find the $\limsup_{t\to\infty}$ on both sides, apply Lemma (1), and factorise to obtain

$$\begin{aligned}\limsup_{t\to\infty} \frac{\ln I_C(t)}{t} &\leq \limsup_{t\to\infty} \frac{\ln I_C(0)}{t} + \Big[\beta_C(1-\kappa\zeta) - (\rho_C + \mu_C) - \frac{\epsilon_3^2}{2} - \mathcal{E}_2\Big] \\ &\quad + \limsup_{t\to\infty} \frac{\mathcal{H}_2(t)}{t} + \limsup_{t\to\infty} \frac{\mathcal{A}_2}{t} \\ &\leq (\rho_C + \mu_c)\Big[\frac{\beta_C(1-\kappa\zeta)}{(\rho_C+\mu_C)} - 1 - \frac{\epsilon_3^2}{2(\rho_C+\mu_C)} - \frac{\mathcal{E}_2}{(\rho_C+\mu_C)}\Big].\end{aligned}$$

From (15) we have

$$\limsup_{t\to\infty} \frac{\ln I_C(t)}{t} \leq (\rho_C + \mu_C)\left(\mathcal{R}_{0C}^s - 1\right).$$

where $\mathcal{H}_2(t) = \int_0^t \epsilon_3 dB_3(t)$, $\mathcal{E}_2 = \int_{\mathcal{U}} (\Psi_2(u) - \ln(1+\Psi_2(u)))v(du)$, and $\mathcal{A}_2 = \int_0^t \int_{\mathcal{U}} \ln(1+\Psi_2(u))\tilde{\mathcal{N}}(ds,du)$ are martingales.
Clearly

$$(\rho_C + \mu_c) > 0.$$

For

$$\lim_{t\to\infty} \sup \frac{\ln I_C(t)}{t} \leq 0.$$

then

$$\mathcal{R}_{0C}^s - 1 < 0.$$

From (1) we conclude that whenever $\mathcal{R}^s_{0C} \leq 1$,

$$\limsup_{t\to\infty} \frac{\ln I_C(t)}{t} \leq 0, \text{ and } \lim_{t\to\infty} I_C(t) = 0.$$

□

3.8 Persistence in Mean

Persistence of a disease means that the disease will remain endemic in the population with positive probability. We study the disease persistence for the system reported in (3) and derive that the disease persists under certain conditions.

Definition 4. *[1] Persistence for Model* (3) *will hold if,*

$$\liminf_{t\to\infty} \frac{1}{t}\int_0^t \mathcal{X}(r)dr \geq 0 \quad a.s.$$

Lemma 2. *[50] Set $g \in \mathbb{C}\big[[0,\infty]\times\Omega,(0,\infty)\big]$, assume that there exist ξ_0, $\xi > 0$ such that*

$$\ln g(t) \geq \xi t - \xi_0 \int_0^t g(s)ds + G(t) \ a.s \quad \forall\, t \geq 0,$$

such that $G \in \big(\mathbb{C}\big[[0,\infty]\times\Omega,(0,\infty)\big]\big)$ satisfying $\lim_{t\to\infty} \frac{G(t)}{t} = 0$ a.s. Then $\lim_{t\to\infty} \langle g(t)\rangle \geq \frac{\xi}{\xi_0} a.s.$

Theorem 15. *Let $(S(t), I_C(t), I_a(t), I_{aC}(t), I_c(t), I_{cC}(t), T_a(t), T_C(t), T_{aC}(t), R_a(t), R_C(t), R_{aC}(t), V_C(t))$ be a solution of system* (3) *with initial values $(S(0), I_C(0), I_a(0), I_{aC}(0), I_c(0), I_{cC}(0), T_a(0), T_C(0), T_{aC}(0), R_a(0), R_C(0), R_{aC}(0), V_C(0)) \in \Omega$.*

1. *If $\mathcal{R}^s_{0a} > 1$ and $\max(\mathcal{R}^s_{0C}, \mathcal{R}^s_{0aC}) < 1$, the disease I_a persists in mean. In addition, I_a satisfies*

$$\lim_{t\to\infty} \langle I_a(t)\rangle \geq (\mu_a + \rho_a)\left(\mathcal{R}^s_{0a} - 1\right).$$

2. *If $\mathcal{R}^s_{0C} > 1$, $\max(\mathcal{R}^s_{0a}\ ,\ \mathcal{R}^s_{0aC}) < 1$, then the disease I_C is persistent in mean. In addition, I_C satisfies*

$$\lim_{t\to\infty} \langle I_C(t)\rangle \geq (\mu_C + \rho_C)\left(\mathcal{R}^s_{0C} - 1\right).$$

Proof. We begin by proving the persistence for co-infection of diseases. Thereafter, using similar techniques, we prove the persistence for singular diseases.

We recall the Itô- Lévy expression of the co-infected equation of (3).

$$\begin{aligned} d\ln I_{aC}(t) = \Bigg[&(\eta_C I_a(t) + \eta_a I_C(t)) - (\rho_{aC} + \theta_{acC} + \mu_{aC}) - \frac{\epsilon_4^2}{2} \\ &+ \int_{\mathcal{U}} (\Psi_3(u) - \ln(1+\Psi_3(u)))v(du)\Bigg]dt + \epsilon_4 dB_4(t) \\ &+ \int_{\mathcal{U}} \ln(1+\Psi_3(u))\tilde{\mathcal{N}}(dt,du). \end{aligned} \tag{54}$$

By integrating both sides of (54) we obtain

$$\begin{aligned}
\int_0^t d\ln I_{aC}(S) &= \eta_C \int_0^t I_a(r)dr + \eta_a \int_0^t I_C(r))dr - \int_0^t \big[(\rho_{aC} + \theta_{acC} + \mu_{aC})\big]dt \\
&\quad - \int_0^t \frac{\epsilon_4^2}{2}dr - \mathcal{E}_3 t + \mathcal{H}_3(t) + \mathcal{A}_3 \\
\ln I_{aC}(t) &= \eta_C \int_0^t I_a(r)dr + \eta_a \int_0^t I_C(r))dr - \big[(\rho_{aC} + \theta_{acC} + \mu_{aC})\big]t \\
&\quad - \frac{\epsilon_4^2}{2}t - \mathcal{E}_3 t + \mathcal{H}_3(t) + \mathcal{A}_3 + \ln I_{aC}(0),
\end{aligned} \tag{55}$$

where $\mathcal{E}_3 = \int_{\mathcal{U}}(\Psi_3(u) - \ln(1 + \Psi_3(u)))v(du)$, $\mathcal{H}_3(t) = \int_0^t \epsilon_4 dB_4(t)$, and $\mathcal{A}_3 = \int_0^t \int_{\mathcal{U}} \ln(1 + \Psi_3(u))\tilde{\mathcal{N}}(ds, du) > 0$. Next we divide through (55) by t, apply comparison and Definition (3) to obtain

$$\begin{aligned}
\frac{\ln I_{aC}(t)}{t} &= \eta_C \frac{1}{t}\int_0^t I_a(r)dr + \eta_a \frac{1}{t}\int_0^t I_C(r))dr - \frac{1}{t}\big[(\rho_{aC} + \theta_{acC} + \mu_{aC})\big]t \\
&\quad - \frac{1}{t}\frac{\epsilon_4^2}{2}t - \frac{1}{t}\mathcal{E}_3 t + \frac{1}{t}\mathcal{H}_3(t) + \frac{1}{t}\mathcal{A}_3 + \frac{\ln I_{aC}(0)}{t} \\
&\geq \eta_C \big\langle I_a(t)\big\rangle + \eta_a \big\langle I_C(t)\big\rangle - \big[(\rho_{aC} + \theta_{acC} + \mu_{aC})\big] - \frac{\epsilon_4^2}{2} - \mathcal{E}_3 \\
&\quad + \frac{\mathcal{H}_3(t)}{t}.
\end{aligned} \tag{56}$$

Next, we determine expressions for $\big\langle I_a(t)\big\rangle$, and $\big\langle I_C(t)\big\rangle$

By integrating the system (3) and dividing by t, to obtain the following:

$$
\begin{cases}
\dfrac{S(t)-S(0)}{t} & = \frac{1}{t}\int_0^t[\psi+\sigma_V V_C(s)+\sigma_{aC}R_{aC}(s)+\sigma_C R_C(s)-(\lambda_a I_a(s) \\
& \quad +\lambda_C I_C(s))S(s)-(\mu+\theta_V)S(s)+\epsilon_1 S(s)dB_1(s) \\
& \quad +\int_{\mathcal{U}}\Psi_1(u)S(s^-)\tilde{\mathcal{N}}(ds,du)] \\
\dfrac{I_a(t)-I_a(0)}{t} & = \frac{1}{t}\int_0^t[\lambda_a I_a(s)S(s)-(\theta_{ac}+\rho_a+\eta_C I_{aC}(s)+\mu_a)I_a(s)+\epsilon_2 I_a(s)dB_2(s)] \\
\dfrac{I_C(t)-I_C(0)}{t} & = \frac{1}{t}\int_0^t[\lambda_C I_C(s)S(s)-(\eta_a I_{aC}(s)+\rho_C+\mu_C)I_C(s)+\epsilon_3 I_C dB_3(s) \\
& \quad +\int_{\mathcal{U}}\Psi_2(u)I_C(s^-)\tilde{\mathcal{N}}(ds,du)] \\
\dfrac{I_{aC}(t)-I_{aC}(0)}{t} & = \frac{1}{t}\int_0^t[(\eta_C I_a(s)+\eta_a I_C(s))I_{aC}(s)-(\rho_{aC}+\theta_{acC}+\mu_{aC})I_{aC})(s) \\
& \quad +\epsilon_4 I_{aC}dB_4(s)+\int_{\mathcal{U}}\Psi_3(u)I_{aC}(s^-)\tilde{\mathcal{N}}(ds,du)] \\
\dfrac{I_c(t)-I_c(0)}{t} & = \frac{1}{t}\int_0^t[\theta_{ac}I_a(s)+\phi_{cC}T_C-(\sigma_c+\mu_c)I_c(s)+\epsilon_5 I_c dB_5(s)] \\
\dfrac{I_{cC}(t)-I_{cC}(0)}{t} & = \frac{1}{t}\int_0^t[\sigma_c I_c(s)+\theta_{acC}I_{aC}-(\mu_{cC}+\rho_{cC})I_{cC}(s)+\epsilon_6 I_{cC}dB_6(s)] \\
\dfrac{T_a(t)-T_a(0)}{t} & = \frac{1}{t}\int_0^t[\rho_a I_a(s)-(\mu+\phi_a)T_a(s)+\epsilon_7 T_a dB_7(s)] \\
\dfrac{T_{aC}(t)-T_{aC}(0)}{t} & = \frac{1}{t}\int_0^t[\rho_{aC}I_{aC}(s)-(\mu+\phi_{aC})T_{aC}(s)+\epsilon_8 T_{aC}dB_8(s)] \\
\dfrac{T_C(t)-T_C(0)}{t} & = \int_0^t[\rho_{cC}I_{cC}(s)+\rho_C I_C(s)-(\mu+\phi_C+\phi_{cC})T_C(s) \\
& \quad +\epsilon_9 T_C dB_9(s)+\int_{\mathcal{U}}\Psi_4(u)T_C(s^-)\tilde{\mathcal{N}}(ds,du)] \\
\dfrac{R_a(t)-R_a(0)}{t} & = \frac{1}{t}\int_0^t[\phi_a T_a(s)-\mu R_a(s)+\epsilon_{10}R_a dB_{10}(s)] \\
\dfrac{R_{aC}(t)-R_{aC}(0)}{t} & = \frac{1}{t}\int_0^t[\phi_{aC}T_{aC}(s)-(\mu+\sigma_{aC})R_{aC}(s)+\epsilon_{11}R_{aC}dB_{11}(s)] \\
\dfrac{R_C(t)-R_C(0)}{t} & = \frac{1}{t}\int_0^t[\phi_C T_C(s)-(\mu+\sigma_C)R_C+\epsilon_{12}R_C dB_{12}(s) \\
& \quad +\int_{\mathcal{U}}\Psi_5(u)R_C(s^-)\tilde{\mathcal{N}}(ds,du)] \\
\dfrac{V_C(t)-V_C(0)}{t} & = \frac{1}{t}\int_0^t[\theta_V S(s)-(\mu+\sigma_V)V_C(s)+\epsilon_{13}V_C dB_{13}(s)],
\end{cases}
\tag{57}
$$

Adding terms and arrange terms of (57), rearranging and applying (3) we obtain

$$
\begin{aligned}
\mu\langle I_a(t)\rangle = \psi - \Big[&\mu\langle S(t)\rangle+\mu\langle I_C(t)\rangle+\mu\langle I_{aC}(t)\rangle+\mu\langle I_c(t)\rangle+\mu\langle I_{cC}\rangle+\mu\langle T_a(t)\rangle \\
&+\mu\langle T_{aC}(t)\rangle+\mu\langle T_C(t)\rangle+\mu\langle R_a(t)\rangle+\mu\langle R_{aC}(t)\rangle+\mu\langle R_C(t)+\mu\langle V_C(t)\rangle\Big] \\
&+\mathbb{Q}(t)-\Big[\frac{S(t)-S(0)}{t}+\frac{I_a(t)-I_a(0)}{t}+\frac{I_C(t)-I_C(0)}{t}+\frac{I_{aC}(t)-I_{aC}(0)}{t} \\
&+\frac{I_c(t)-I_c(0)}{t}+\frac{I_{cC}(t)-I_{cC}(0)}{t}+\frac{T_a(t)-T_a(0)}{t}+\frac{T_{aC}(t)-T_{aC}(0)}{t} \\
&+\frac{T_C(t)-T_C(0)}{t}+\frac{R_a(t)-R_a(0)}{t}+\frac{R_{aC}(t)-R_{aC}(0)}{t}+\frac{R_C(t)-R_C(0)}{t} \\
&+\frac{V_C(t)-V_C(0)}{t}+\mathbb{Z}(t)\Big],
\end{aligned}
\tag{58}
$$

and

$$
\begin{aligned}
\mu\big\langle I_C(t)\big\rangle = \psi - \Big[&\mu\big\langle S(t)\big\rangle + \mu\big\langle I_a(t)\big\rangle + \mu\big\langle I_{aC}(t)\big\rangle + \mu\big\langle I_c(t)\big\rangle + \mu\big\langle I_{cC}\big\rangle + \mu\big\langle T_a(t)\big\rangle \\
&+ \mu\big\langle T_{aC}(t)\big\rangle + \mu\big\langle T_C(t)\big\rangle + \mu\big\langle R_a(t)\big\rangle + \mu\big\langle R_{aC}(t)\big\rangle + \mu\big\langle R_C(t) + \mu\big\langle V_C(t)\big\rangle\Big] \\
&+ \mathbb{Q}(t) - \Big[\frac{S(t)-S(0)}{t} + \frac{I_a(t)-I_a(0)}{t} + \frac{I_C(t)-I_C(0)}{t} + \frac{I_{aC}(t)-I_{aC}(0)}{t} \\
&+ \frac{I_c(t)-I_c(0)}{t} + \frac{I_{cC}(t)-I_{cC}(0)}{t} + \frac{T_a(t)-T_a(0)}{t} + \frac{T_{aC}(t)-T_{aC}(0)}{t} \\
&+ \frac{T_C(t)-T_C(0)}{t} + \frac{R_a(t)-R_a(0)}{t} + \frac{R_{aC}(t)-R_{aC}(0)}{t} + \frac{R_C(t)-R_C(0)}{t} \\
&+ \frac{V_C(t)-V_C(0)}{t} + \mathbb{Z}(t)\Big],
\end{aligned}
\tag{59}
$$

where

$$
\begin{aligned}
\mathbb{Q} = &\frac{\epsilon_1}{t}\int_0^t S(s)dB_1(s) + \frac{\epsilon_2}{t}\int_0^t I_a(s)dB_2(s) + \frac{\epsilon_3}{t}\int_0^t I_C(s)dB_3(s) \\
&+ \frac{\epsilon_4}{t}\int_0^t I_{aC}(s)dB_4(s) + \frac{\epsilon_5}{t}\int_0^t I_c(s)dB_5(s) + \frac{\epsilon_6}{t}\int_0^t I_{cC}(s)dB_6(s) \\
&+ \frac{\epsilon_7}{t}\int_0^t T_a(s)dB_7(s) + \frac{\epsilon_8}{t}\int_0^t T_{aC}(s)dB_8(s) + \frac{\epsilon_9}{t}\int_0^t T_C(s)dB_9(s) \\
&+ \frac{\epsilon_{10}}{t}\int_0^t R_a(s)dB_{10}(s) + \frac{\epsilon_{11}}{t}\int_0^t RaC(s)dB_{11}(s) + \frac{\epsilon_{12}}{t}\int_0^t R_C(s)dB_{12}(s) \\
&+ \frac{\epsilon_{13}}{t}\int_0^t V_C(s)dB_{13}(s)
\end{aligned}
$$

$$
\mathbb{Z}(t) = \frac{1}{t}\int_0^t\int_{\mathcal{U}}\Big[\sum_{i=1}^{5}\psi_i(u)\nabla_i(t^-)\tilde{\mathcal{N}}(ds,du)\Big],
$$

and $(\nabla_1, \nabla_2, \nabla_3, \nabla_4, \nabla_5) = (S, I_C, I_{aC}, T_C, R_C)$. We substitute (58) and (59) into (56), take $\liminf_{t\to\infty}$, eliminate $\mathbb{Z}(t)$, and apply the strong law of martingales (i.e. Lemma (1)) to get

$$
\begin{aligned}
\frac{\ln I_{aC}(t)}{t} \geq\ & \eta_C \frac{1}{\mu}\Big[\psi - \Big[\mu\big\langle S(t)\big\rangle + \mu\big\langle I_C(t)\big\rangle + \mu\big\langle I_{aC}(t)\big\rangle + \mu\big\langle I_c(t)\big\rangle + \mu\big\langle I_{cC}\big\rangle + \mu\big\langle T_a(t)\big\rangle \\
& + \mu\big\langle T_{aC}(t)\big\rangle + \mu\big\langle T_C(t)\big\rangle + \mu\big\langle R_a(t)\big\rangle + \mu\big\langle R_{aC}(t)\big\rangle + \mu\big\langle R_C(t) + \mu\big\langle V_C(t)\big\rangle\Big] \\
& + \mathbb{Q}(t) - \Big[\frac{S(t)-S(0)}{t} + \frac{I_a(t)-I_a(0)}{t} + \frac{I_C(t)-I_C(0)}{t} + \frac{I_{aC}(t)-I_{aC}(0)}{t} \\
& + \frac{I_c(t)-I_c(0)}{t} + \frac{I_{cC}(t)-I_{cC}(0)}{t} + \frac{T_a(t)-T_a(0)}{t} + \frac{T_{aC}(t)-T_{aC}(0)}{t} \\
& + \frac{T_C(t)-T_C(0)}{t} + \frac{R_a(t)-R_a(0)}{t} + \frac{R_{aC}(t)-R_{aC}(0)}{t} + \frac{R_C(t)-R_C(0)}{t} \\
& + \frac{V_C(t)-V_C(0)}{t}\Big]\Big] + \eta_a \frac{1}{\mu}\Big[\psi - \Big[\mu\big\langle S(t)\big\rangle + \mu\big\langle I_C(t)\big\rangle + \mu\big\langle I_{aC}(t)\big\rangle + \mu\big\langle I_c(t)\big\rangle \\
& + \mu\big\langle I_{cC}\big\rangle + \mu\big\langle T_a(t)\big\rangle + \mu\big\langle T_{aC}(t)\big\rangle + \mu\big\langle T_C(t)\big\rangle + \mu\big\langle R_a(t)\big\rangle + \mu\big\langle R_{aC}(t)\big\rangle \\
& + \mu\big\langle R_C(t) + \mu\big\langle V_C(t)\big\rangle\Big] + \mathbb{Q}(t) - \Big[\frac{S(t)-S(0)}{t} + \frac{I_a(t)-I_a(0)}{t} \\
& + \frac{I_C(t)-I_C(0)}{t} + \frac{I_{aC}(t)-I_{aC}(0)}{t} + \frac{I_c(t)-I_c(0)}{t} + \frac{I_{cC}(t)-I_{cC}(0)}{t} \\
& + \frac{T_a(t)-T_a(0)}{t} + \frac{T_{aC}(t)-T_{aC}(0)}{t} + \frac{T_C(t)-T_C(0)}{t} + \frac{R_a(t)-R_a(0)}{t} \\
& + \frac{R_{aC}(t)-R_{aC}(0)}{t} + \frac{R_C(t)-R_C(0)}{t} + \frac{V_C(t)-V_C(0)}{t}\Big]\Big] - (\rho_{aC} + \theta_{acC} \\
& + \mu_{aC}) - \frac{\epsilon_4^2}{2} - \mathcal{E}_3 + \frac{\mathcal{H}_3(t)}{t} + \frac{\mathcal{A}_3}{t} + \frac{\ln I_{aC}(0)}{t} + \frac{\ln I_{aC}(0)}{t}.
\end{aligned} \tag{60}
$$

Next, find $\liminf_{t\to\infty}$ and apply a Lemma (2) and definition (4) to obtain following results,

$$\begin{aligned}
\liminf_{t\to\infty}\frac{\ln I_{aC}(t)}{t} \geq \liminf_{t\to\infty}\Bigg(&\eta_C\frac{1}{\mu}\Big[\psi-\Big[\mu\big\langle S(t)\big\rangle+\mu\big\langle I_C(t)\big\rangle+\mu\big\langle I_{aC}(t)\big\rangle+\mu\big\langle I_c(t)\big\rangle\\
&+\mu\big\langle I_{cC}\big\rangle+\mu\big\langle T_a(t)\big\rangle+\mu\big\langle T_{aC}(t)\big\rangle+\mu\big\langle T_C(t)\big\rangle+\mu\big\langle R_a(t)\big\rangle+\mu\big\langle R_{aC}(t)\big\rangle\\
&+\mu\big\langle R_C(t)+\mu\big\langle V_C(t)\big\rangle\Big]+\mathbb{Q}(t)-\Big[\frac{S(t)-S(0)}{t}+\frac{I_a(t)-I_a(0)}{t}\\
&+\frac{I_C(t)-I_C(0)}{t}+\frac{I_{aC}(t)-I_{aC}(0)}{t}+\frac{I_c(t)-I_c(0)}{t}+\frac{I_{cC}(t)-I_{cC}(0)}{t}\\
&+\frac{T_a(t)-T_a(0)}{t}+\frac{T_{aC}(t)-T_{aC}(0)}{t}+\frac{T_C(t)-T_C(0)}{t}+\frac{R_a(t)-R_a(0)}{t}\\
&+\frac{R_{aC}(t)-R_{aC}(0)}{t}+\frac{R_C(t)-R_C(0)}{t}+\frac{V_C(t)-V_C(0)}{t}\Big]\Big]+\eta_a\frac{1}{\mu}\Big[\psi\\
&-\Big[\mu\big\langle S(t)\big\rangle+\mu\big\langle I_C(t)\big\rangle+\mu\big\langle I_{aC}(t)\big\rangle+\mu\big\langle I_c(t)\big\rangle+\mu\big\langle I_{cC}\big\rangle+\mu\big\langle T_a(t)\big\rangle\\
&+\mu\big\langle T_{aC}(t)\big\rangle+\mu\big\langle T_C(t)\big\rangle+\mu\big\langle R_a(t)\big\rangle+\mu\big\langle R_{aC}(t)\big\rangle+\mu\big\langle R_C(t)+\mu\big\langle V_C(t)\big\rangle\Big]\\
&+\mathbb{Q}(t)-\Big[\frac{S(t)-S(0)}{t}+\frac{I_a(t)-I_a(0)}{t}+\frac{I_C(t)-I_C(0)}{t}+\frac{I_{aC}(t)-I_{aC}(0)}{t}\\
&+\frac{I_c(t)-I_c(0)}{t}+\frac{I_{cC}(t)-I_{cC}(0)}{t}+\frac{T_a(t)-T_a(0)}{t}+\frac{T_{aC}(t)-T_{aC}(0)}{t}\\
&+\frac{T_C(t)-T_C(0)}{t}+\frac{R_a(t)-R_a(0)}{t}+\frac{R_{aC}(t)-R_{aC}(0)}{t}+\frac{R_C(t)-R_C(0)}{t}\\
&+\frac{V_C(t)-V_C(0)}{t}\Big]\Big]-(\rho_{aC}+\theta_{acC}+\mu_{aC})-\frac{\epsilon_4^2}{2}+\epsilon_4\frac{1}{t}\int_0^t dB_4(t)\\
&+\frac{1}{t}\int_0^t\int_{\mathcal{U}}\ln(1+\Psi_2(u))\tilde{\mathcal{N}}(dt,du)+\frac{\ln I_{aC}(0)}{t}\Bigg)\\
\geq&\left[\frac{\eta_C\psi}{\mu}+\frac{\eta_a\psi}{\mu}-(\rho_{aC}+\theta_{acC}+\mu_{aC})-\frac{\epsilon_4^2}{2}\right]\\
\geq&(\rho_{aC}+\theta_{acC}+\mu_{aC})\Big[\frac{\beta_C(1-\kappa\zeta)}{\mathbf{G}}+\frac{\beta_a(1-\kappa\zeta)}{\mathbf{G}}-1-\frac{\epsilon_4^2}{2\mathbf{G}}\Big].
\end{aligned}$$

From (45) we have

$$\liminf_{t\to\infty}\frac{\ln I_{aC}(t)}{t}\geq(\rho_{aC}+\theta_{acC}+\mu_{aC})\Big[\mathcal{R}_{0aC}^s-1\Big].$$

Clearly,

$$(\eta+\mu+\rho_{HC})>0.$$

If

$$\lim_{t\to\infty}\inf\frac{\ln I_{aC}(t)}{t}\geq 0,$$

then

$$\mathcal{R}_{0aC}^s-1>0.$$

By Definition (4) Lemma (2), we conclude that whenever $\mathcal{R}^s_{0aC} > 1$,

$$\begin{aligned}\lim_{t\to\infty}\langle I_{aC}(t)\rangle &\geq \lim_{t\to\infty}\inf\langle I_{aC}(t)\rangle \geq \liminf_{t\to\infty}\frac{\ln I_{aC}(t)}{t}\\ &\geq (\eta+\mu+\rho_{aC})\,(\mathcal{R}^s_{0aC}-1) > 0.\end{aligned}$$

Next, we prove the persistence for HBV only Model. By rearranging terms in (59), we get

$$\begin{aligned}\mu\big\langle S(t)\big\rangle = \psi - \Big[&\mu\big\langle I_C(t)\big\rangle + \mu\big\langle I_a(t)\big\rangle + \mu\big\langle I_{aC}(t)\big\rangle + \mu\big\langle I_c(t)\big\rangle + \mu\big\langle I_{cC}\big\rangle + \mu\big\langle T_a(t)\big\rangle\\ &+ \mu\big\langle T_{aC}(t)\big\rangle + \mu\big\langle T_C(t)\big\rangle + \mu\big\langle R_a(t)\big\rangle + \mu\big\langle R_{aC}(t)\big\rangle + \mu\big\langle R_C(t) + \mu\big\langle V_C(t)\big\rangle\Big]\\ &+ \mathbb{Q}(t) - \Big[\frac{S(t)-S(0)}{t} + \frac{I_a(t)-I_a(0)}{t} + \frac{I_C(t)-I_C(0)}{t} + \frac{I_{aC}(t)-I_{aC}(0)}{t}\\ &+ \frac{I_c(t)-I_c(0)}{t} + \frac{I_{cC}(t)-I_{cC}(0)}{t} + \frac{T_a(t)-T_a(0)}{t} + \frac{T_{aC}(t)-T_{aC}(0)}{t}\\ &+ \frac{T_C(t)-T_C(0)}{t} + \frac{R_a(t)-R_a(0)}{t} + \frac{R_{aC}(t)-R_{aC}(0)}{t} + \frac{R_C(t)-R_C(0)}{t}\\ &+ \frac{V_C(t)-V_C(0)}{t}\Big].\end{aligned} \tag{61}$$

Next, we integrate both sides of (29), and eliminate positive terms to get

$$\begin{aligned}\ln I_a(t) - \ln I_a(0) &= \lambda_a\int_0^t S(t)dr - \int_0^t(\rho_a+\mu_a+\theta_{ac})dr - \int_0^t\frac{\epsilon_2^2}{2}dr + \int_0^t\epsilon_2 dB_2(t)\\ \ln I_a(t) &\geq \lambda_a\int_0^t S(t)dr - \int_0^t(\rho_a+\mu_a+\theta_{ac})dr - \int_0^t\frac{\epsilon_2^2}{2}dr + \int_0^t\epsilon_2 dB_2(t).\end{aligned} \tag{62}$$

We divide (62) by t, substitute (61) into (62), to get

$$\begin{aligned}\frac{\ln I_a(t)}{t} &\geq \lambda_a\frac{1}{t}\int_0^t S(t)dr - \frac{1}{t}\int_0^t(\rho_a+\mu_a+\theta_{ac})dr - \frac{1}{t}\int_0^t\frac{\epsilon_2^2}{2}dr + \frac{1}{t}\int_0^t\epsilon_2 dB_2(t)\\ &= \frac{\beta_a\mu(1-\kappa\zeta)}{\mu\psi}\Big[\psi - \Big[\mu\big\langle I_C(t)\big\rangle + \mu\big\langle I_a(t)\big\rangle + \mu\big\langle I_{aC}(t)\big\rangle + \mu\big\langle I_c(t)\big\rangle + \mu\big\langle I_{cC}\big\rangle\\ &+ \mu\big\langle T_a(t)\big\rangle + \mu\big\langle T_{aC}(t)\big\rangle + \mu\big\langle T_C(t)\big\rangle + \mu\big\langle R_a(t)\big\rangle + \mu\big\langle R_{aC}(t)\big\rangle + \mu\big\langle R_C(t)\\ &+ \mu\big\langle V_C(t)\big\rangle\Big] + \mathbb{Q}(t) - \Big[\frac{S(t)-S(0)}{t} + \frac{I_a(t)-I_a(0)}{t} + \frac{I_C(t)-I_C(0)}{t}\\ &+ \frac{I_{aC}(t)-I_{aC}(0)}{t} + \frac{I_c(t)-I_c(0)}{t} + \frac{I_{cC}(t)-I_{cC}(0)}{t} + \frac{T_a(t)-T_a(0)}{t}\\ &+ \frac{T_{aC}(t)-T_{aC}(0)}{t} + \frac{T_C(t)-T_C(0)}{t} + \frac{R_a(t)-R_a(0)}{t} + \frac{R_{aC}(t)-R_{aC}(0)}{t}\\ &+ \frac{R_C(t)-R_C(0)}{t} + \frac{V_C(t)-V_C(0)}{t}\Big] - (\rho_a+\mu_a+\theta_{ac})\\ &- \frac{1}{2}\epsilon_2^2 + \frac{1}{t}\int_0^t\epsilon_2 dB_2(t).\end{aligned} \tag{63}$$

We find $\liminf_{t\to\infty}$ and apply Definition (4) and Lemma (2) to get

$$\begin{aligned}\liminf_{t\to\infty}\frac{\ln I_a(t)}{t} &\geq \beta_a(1-\kappa\zeta)-(\rho_a+\mu_a+\theta_{ac})-\frac{1}{2}\epsilon_2^2\\ &= (\rho_a+\mu_a+\theta_{ac})\left[\frac{\beta_a(1-\kappa\delta)}{(\rho_a+\mu_a+\theta_{ac})}-1-\frac{\epsilon_2^2}{2(\rho_a+\mu_a+\theta_{ac})}\right].\end{aligned}$$

From (29) we have

$$\liminf_{t\to\infty}\frac{\ln I_a(t)}{t} \geq (\rho_a+\mu_a+\theta_{ac})\Big[\mathcal{R}_{0a}^s-1\Big].$$

Clearly,

$$(\rho_a+\mu_a+\theta_{ac})>0.$$

If

$$\liminf_{t\to\infty}\frac{\ln I_a(t)}{t}\geq 0,$$

then

$$\mathcal{R}_{0a}^s-1>0.$$

By Definition (4) and Lemma (2), we conclude that whenever $\mathcal{R}_{0a}^s>1$,

$$\begin{aligned}\lim_{t\to\infty}\langle I_a(t)\rangle \geq \lim_{t\to\infty}\inf\langle I_a(t)\rangle &\geq \liminf_{t\to\infty}\frac{\ln I_a(t)}{t}\\ &\geq (\rho_a+\mu_a+\theta_{ac})\left(\mathcal{R}_{0a}^s-1\right)>0.\end{aligned}$$

Next, we prove the persistence in mean for COVID-19. We recall the Itô- Lévy expression of the COVID-19 infected equation of (3)

$$\begin{aligned}d\ln I_C(t) = &\Big[\lambda_C S(t)-(\rho_C+\mu_C)-\frac{\epsilon_3^2}{2}-\int_{\mathcal{U}}(\Psi_1(u)-\ln(1+\Psi_3(u)))v(du)\Big]dt\\ &+\epsilon_3 dB_3(t)+\int_{\mathcal{U}}(\ln(1+\Psi_1(u))\tilde{\mathcal{N}}(dt,du).\end{aligned}$$

Integrating both sides we obtain

$$\begin{aligned}\ln I_C(t)-\ln I_C(0) = &\lambda_C\int_0^t S(r)dr-\int_0^t\Big(\rho_C+\mu_C+\frac{\epsilon_3^2}{2}\Big)dr+\int_0^t\epsilon_3 dB_3(r)\\ &-\int_0^t\int_{\mathcal{U}}(\Psi_1(u)-\ln(1+\Psi_1(u)))v(du)dr\\ &+\int_0^t\int_{\mathcal{U}}\ln(1+\Psi_1(u))\tilde{\mathcal{N}}(ds,du).\end{aligned}\tag{64}$$

We divide (64) by t, substitute (61) into (64) to get,

$$\begin{aligned}\frac{\ln I_C(t)}{t} &\geq \lambda_C \frac{1}{t}\int_0^t S(r)dr - (\rho_C+\mu_C) - \frac{1}{2}\epsilon_3^2 - \mathcal{E}_2 + \limsup_{t\to\infty}\frac{\mathcal{H}_2(t)}{t} + \limsup_{t\to\infty}\frac{\mathcal{A}_2}{t}\\ &\geq \frac{\beta_C(1-\kappa\zeta)\mu}{\mu\psi}\Bigg[\psi - \Bigg[\mu\big\langle I_a(t)\big\rangle + \mu\big\langle I_C(t)\big\rangle + \mu\big\langle i_{aC}(t)\big\rangle + \mu\big\langle R(t)\big\rangle\\ &\quad + \mu\big\langle V(t)\big\rangle\Bigg] + \mathbb{Q}(t) - \Bigg[\frac{(S(t)-S(0))}{t} + \frac{(I_C(t)-I_C(0))}{t}\\ &\quad + \frac{(T_C(t)-T_C(0))}{t} + \frac{(R_C(t)-R_C(0))}{t} + \frac{(V_C(t)-V_C(0))}{t}\Bigg]\Bigg]\\ &\quad - (\rho_C+\mu_C) - \frac{1}{2}\epsilon_3^2 - \mathcal{E}_2 + \limsup_{t\to\infty}\frac{\mathcal{H}_2(t)}{t} + \limsup_{t\to\infty}\frac{\mathcal{A}_2}{t},\end{aligned} \tag{65}$$

where $\mathcal{H}_2(t) = \int_0^t \epsilon_3 dB_3(t)$, $\mathcal{E}_2 = \int_{\mathcal{U}}(\Psi_1(u) - \ln(1+\Psi_1(u)))v(du)$, and $\mathcal{A}_2 = \int_0^t\int_{\mathcal{U}}\ln(1+\Psi_1(u))\tilde{\mathcal{N}}(ds,du)$ are martingales. We take $\liminf_{t\to\infty}$ of both sides and apply Definition (4) and Lemma (2) to get

$$\begin{aligned}\liminf_{t\to\infty}\frac{\ln I_C(t)}{t} &\geq \beta_C(1-\kappa\zeta) - (\rho_C+\mu_C) - \frac{\epsilon_2^2}{2} - \mathcal{E}_2\\ &= (\rho_C+\mu_C)\Bigg[\frac{\beta_C(1-\kappa\zeta)}{(\rho_C+\mu_C)} - 1 - \frac{\epsilon_2^2}{2(\rho_C+\mu_C)} - \frac{\mathcal{E}_2}{(\rho_C+\mu_C)}\Bigg].\end{aligned}$$

From (15) we have

$$\liminf_{t\to\infty}\frac{\ln I_C(t)}{t} \geq (\rho_C+\mu_C)\Big[\mathcal{R}_{0C}^s - 1\Big].$$

Clearly,

$$(\rho_C+\mu_C) > 0.$$

If

$$\liminf_{t\to\infty}\frac{\ln I_C(t)}{t} \geq 0,$$

then

$$\mathcal{R}_{0C}^s - 1 > 0.$$

Using Definition (4) and Lemma (2), we conclude that whenever $\mathcal{R}_{0C}^s > 1$,

$$\lim_{t\to\infty}\langle I_C(t)\rangle \geq \lim_{t\to\infty}\inf\langle I_C(t)\rangle \geq (\rho_C+\mu_C)\left(\mathcal{R}_{0C}^s - 1\right) > 0.$$

□

4 Numerical Results

In this section, we employ a standard numerical procedure to obtain numerical simulation results for the HBV-only, COVID-19-only, and HBV-COVID-19 co-infection models. The objective here is to demonstrate the theoretical results obtained earlier in this thesis.

The estimated parameters in Table (1) were derived using a combination of publicly available epidemiological data (e.g., Ghana Health Service reports, WHO reports, and peer-reviewed studies

on COVID-19 and HBV), mathematical approximations using known biological and epidemiological relationships, and reasonable assumptions based on parameter values reported in similar studies when direct Ghana-specific data was unavailable.

At the beginning of the COVID-19 spread in Ghana (early 2020), the birth rate was approximately 28.60 births per 1,000 people [27]. This gives us an estimate for recruitment rate, $\psi = 0.0286$ per person.

An estimate for the natural death rate μ was determined using, Ghana's life expectancy of (64.5 years) and formula

$$\mu = \frac{1}{\text{Life Expectancy}} = \frac{1}{64.5} = 0.0155 \text{ per year} \approx 0.02 \text{ per year.}$$

The approximation was based on published rate from other Ghanaian studies , see, e.g., [25].

COVID-19 death rate was estimated using $\mu_C = \mu + \gamma$. Available data from Ghana, shows that as of March 28, 2022 there were 1,445 COVID-19 related deaths and 161,370 confirmed COVID-19 cases [53]. Thus, the estimated COVID-19 induced death rate is

$$\gamma = \frac{\text{Total COVID-19 deaths}}{\text{Total COVID-19 cases}} = \frac{1,445}{161,370} \approx 0.0089 \text{ deaths per case.}$$

Thus, $\mu_C = \mu + \gamma = 0.02 + 0.0089$ per case.

To estimate the death rate in HBV, we first estimate the additional induced rate

$$d = \frac{\text{Total HBV-related deaths}}{\text{Total HBV-infected population}}.$$

From epidemiological studies, Ghana's HBV prevalence is estimated at 8.48% 12.30% , see, e.g., [68]. Assuming a population of 32 million, the HBV-infected population would be HBV cases $= 32,000,000 \times 0.011 = 3,520,600$. According to [21], in 2022, over 15,000 people in Ghana died from hepatitis B and C-related liver diseases. Thus, the induced death rate was estimated as $d = \frac{15,000}{3,520,000} \approx 0.0042$. Hence the death rate in HBC state is estimated as $\mu_a = \mu + d = 0.02 + 0.004$ per case. With regards to COVID-19 recovery rate, it has been reported that mild cases of COVID-19 typically resolve within 10–14 days COVID-19 [12]. We estimated the recovery rate as $\phi_C = \frac{1}{\text{average infectious period}} \approx 0.07$ per day. We scaled the value by 3 to reflect high recoveries in Ghana and to reflect published regional COVID-19 recovery rates , see, e.g., [17].

Acute HBV Recovery occurs over weeks to months [11]. We use and average infectious period of 60–180 days, to estimate the recovery rate as $\phi_a = \frac{1}{90} = 0.0111$ per day

The parameter values used along with their sources are displayed in Table 2, few values of other parameters were assumed. We sought to verify theoretical results, we selected initial values of $S(0) = 100, I_C(0) = 20, I_a(0) = 20, I_{aC}(0) = 5, I_c(0) = 2, I_{cC}(0) = 0, T_a(0) = 3, T_C(0) = 0; T_{aC}(0) = 0, R_a(0) = 2, R_C(0) = 0, R_{aC}(0) = 0, V_C(0) = 0$. The Euler-Maruyana scheme presented by [33] was employed in conducting the numerical simulations for all models. The results from numerical simulation for HBV only, COVID-19 only and confection model are presented in Figures 3 - 12.

Table 2: Parameters and description

Parameter	value	source
ψ	0.028 births per year	[27]
θ_{ac}	0.033 per day	Estimated [13]
θ_{acC}	0.053 per day	Estimated [13].
β_C	$[0.4800, 0.6500]$ per day	[14] [16]
β_a	0.4 per day	Estimated [68]
ρ_a	0.05 per day	Assumed
ρ_{aC}	$\frac{1}{6}$	Assumed
ρ_C	$\frac{1}{6}$	Estimated [40]
ρ_{cC}	$\frac{1}{13}$	Estimated [40]
ϕ_{aC}	0.3 per day	Estimated [3]
ϕ_a	≈ 0.05 per day	Estimated
ϕ_C	0.2	[17, 7]
ϕ_{cC}	0.03 per day	Estimated
σ_V	0.01 no unit	[35]
σ_C	0.0110	[42]
σ_{aC}	0.002	Assumed
θ_V	0.10	[9]
μ	0.02	[25]
μ_C	0.028 per case	Estimated [25]
μ_{aC}	0.03 per case	Assumed
μ_a	0.021 per case	Estimated
μ_c	0.024 per case	Estimated
μ_{cC}	0.03 per case	Assumed
κ	[0-1]	Assumed
δ	[0-1]	Assumed
ζ	[0-1]	Assumed

4.1 Hepatitis B Virus Only Model

From the parameter values in Table 2, we calculated the reproductive number of HBV model to be $\mathcal{R}_{0a}^d = 1.934$. The result implies that on the average, an infected person introduced into the population can infect more than one susceptible, hence, the infection will continue. This result is consistent with other Ghanaian studies. [60] estimated the value of the Reproductive Number of HBV as $\mathcal{R}_{0a} = 1.957$, thus suggesting an epidemic population. The trajectories of susceptible, infectious, treatment and recovered classes in the HBV-only model (3) are displayed in Figure 3. Here, we fixed values of all parameters shown in Table 2.

From Figure 3, we observed that as number of infectious population increase in time, the susceptible population decrease. However, in the long run, the solution curves for both the susceptible and infective compartments behave like decreasing functions and approach a fixed point. A decrease in the number of susceptible individuals occurred rapidly within the first fifteen time steps of the epidemic, after which there was gradual decline over time. We also observe a sharp increase in the number of HBV infective within the first ten time steps and a relatively gradual increase in the number of individuals in the Treatment (or hospitalised) and other compartments within the same period. Eventually, infectious, recovered classes and other classes approach a fixed

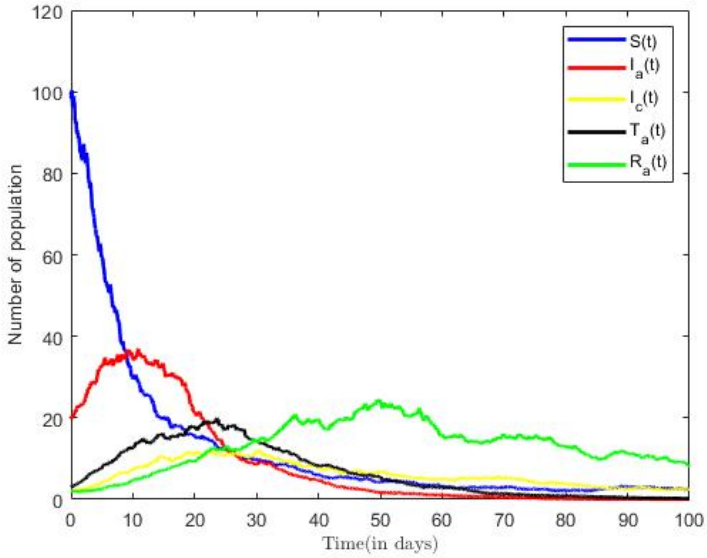

Figure 3: Solution for HBV Only Model ($\delta = 0.7, \zeta = 0.6$).

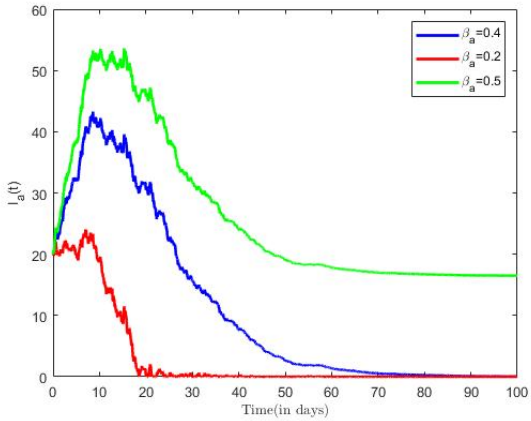

Figure 4: HBV Infection with varied effective contact rate.

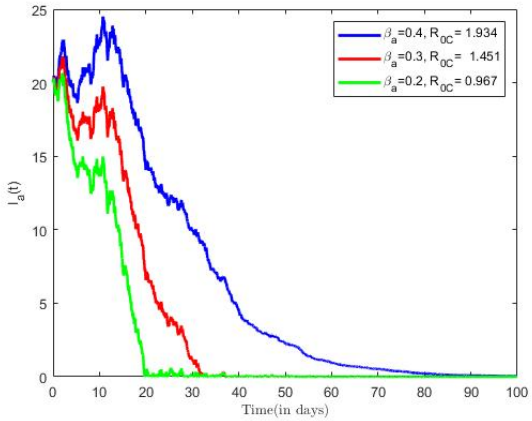

Figure 5: Infected population with varied transmission rate.

point in the long run. In other words, the results suggest that all compartments will reach their respective endemic fixed point of model (28) within a finite time and in long run. The numerical outcomes verifies that when $\mathcal{R}^s_{0a} > 1$, then the disease endemic equilibrium is locally and globally asymptotically stable.

The impact of various parameters on the transmission dynamics of HBV is explored. Numerical results are presented in Figure 4.We proceeded by first investigating the effects of transmission rate on population of infected individuals. This was done using selected values of transmission rates ($\beta_a = 0.4, 0.3, 0.2$), while all remaining parameter values of the model were held constant. From Figure 4, we observe that as values of transmission rate increases, there is an increased possibility for the population to be infected by HBV, and vice versa. Next, we investigated the effects of the transmission rate on the reproductive number of the HBV only model. Here, we held all other parameters constant, and decreased the transmission rates ($\beta_a = 0.4$, 0.3, 0.2). Using the varied transmission rate, we estimated Reproductive numbers as 1.934, 1.451, and 0.967 respectively. We

observe from Figure 5, that for $\mathcal{R}_{0a}^{d} < 1$, the number of infected individuals already introduced into the population declined rapidly to a zero disease free equilibrium point. The observation implies that at $\mathcal{R}_{0a}^{d} < 1$, the disease will eventually become extinct. Further, it is observed from Figure 5 that an increase in the transmission rates from $\beta_a = 0.3$ to $\beta_a = 0.4$ led to increases in the Reproductive number, which translates into increases in the number of infective population over time, as well as an increase in the time to endemic equilibrium. Numerical simulations of the model in Figure 5 suggest that decreasing increasing compliance to protective measures or the decreasing disease transmission rates results in a reduction of $\mathcal{R}_{0a}^{d}$, thus, reduces the average number of HBV infections in the population leading to extinction of the disease. We therefore suggest that all persons comply to preventive measures including vaccination, safe sexual practices, desist from the sharing syringes, ensuring healthcare providers use sterile, single-use needles and screen blood donations screened HBV.

4.2 COVID-19 Only Model

From the parameter values in Table 2, we calculated the reproductive number of COVID-19 of Ghana as $\mathcal{R}_{0C}^{d} = 1.4892$, for a transmission rate on $\beta_C = 0.5$. The result implies that on the average, an infected person introduced into the population can infect more than one susceptible, hence, the infection will continue. This result is consistent with other Ghanaian studies , see, e.g., [54, 14]. According to [14] the estimated the value of the Reproductive number of COVID-19 in Ghana ranges between $\mathcal{R}_{0C} = 1.47$ and $\mathcal{R}_{0C} = 2.65$ for transmission rates of 0.5 and 0.9 respective, thus suggesting an epidemic population at these rates of transmission. The trajectories of susceptible, infectious, vaccinated and recovered classes in the COVID-only model (11) with only with both noise and with only Brownian noise are displayed in Figure 6 and Figure 7 respectively. Here, we fixed values of all parameters shown in Table 2.

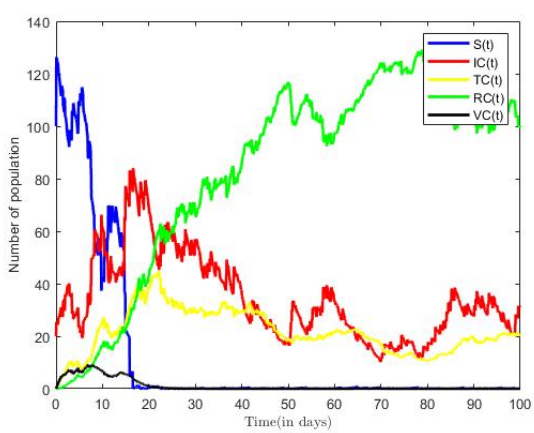

Figure 6: Solution to COVID-19 Only Model with both Noise ($\beta = 0.5, \kappa = 0.5, \zeta = 0.4$).

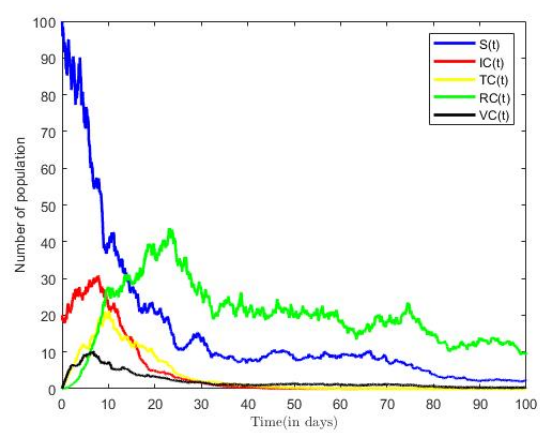

Figure 7: Solution to COVID-19 Only Model with Brownian noise($\beta = 0.5, \kappa = 0.5, \zeta = 0.4$).

From Figure 7, we observed that as number of infectious population increase in time, the susceptible population decrease. However, in the long run, the solution curves for both the susceptible and infective compartments behave like decreasing functions and approach a fixed point. A decrease in the number of susceptible individuals occurred rapidly within the first twenty-five time steps of the epidemic, after which there was gradual decline over time. The pattern was more rapid

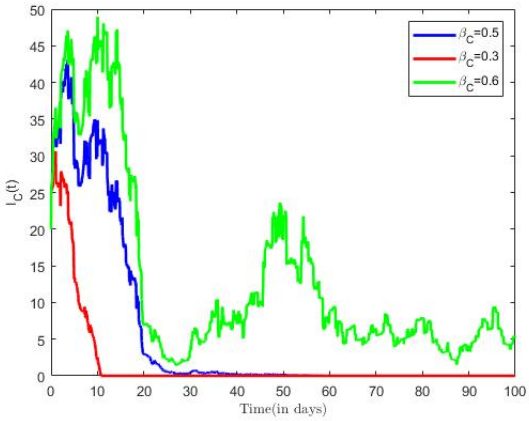

Figure 8: Solution to COVID-19 Only Model with Both Noise ($\beta = 0.5, \kappa = 0.5, \zeta = 0.4$.

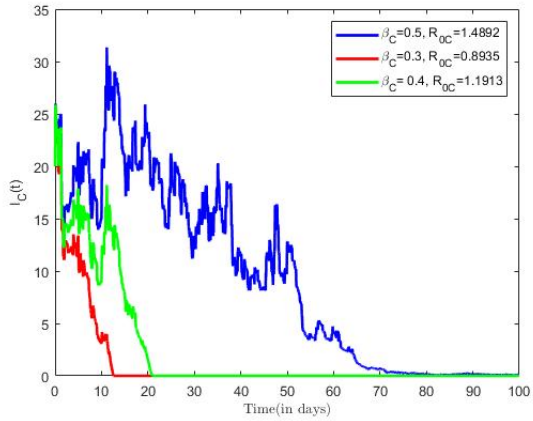

Figure 9: Solution to COVID-19 Only Model with Both Noise ($\beta = 0.5, \kappa = 0.5, \zeta = 0.4$).

in Figure 6 occurring within fifteen time steps. From Figure 7, we also observe a sharp increase in the number of COVID-19 infective within the first ten time steps and a relatively gradual increase in the number of individuals in the Treatment(or hospitalised) and other compartments within the same period. Eventually, infectious, recovered, and other classes in Figure 7 approach a fixed point in the long run. In other words, the results suggest that all compartments will reach their respective endemic fixed point of model (11) within a finite time and in long run. The numerical outcomes verifies that when $\mathcal{R}^s_{0C} > 1$, the disease endemic equilibrium is locally and globally asymptotically stable. It is worth nothing that the number of infective and time to reach endemic fixed point were greatly influenced by the inclusion of Lévy jumps in the COVID-19 only model 7.

The impact of various parameters on the transmission dynamics of COVID-19 is explored. Numerical results are presented in Figure 8 and Figure 9. We proceeded by first investigating the effects of transmission rate on population of infected individuals. This was done using selected values of transmission rates ($\beta_C = 0.3, 0.5, 0.6$), while all remaining parameter values of the model were held constant. From Figure 8, we observe that as values of transmission rate increases, there is an increased possibility for the population to be infected by COVID-19, and vice versa.

Next, we investigated the effects of the transmission rate on the reproductive number of the COVID-19 only model. Here, we held all other parameters constant, and decreased the transmission rates $\beta_C = (0.3,\ 0.5,\ 0.6)$. Using the varied transmission rates, we estimated Reproductive numbers as 0.8935, 1.1913, and 1.4894 respectively. We observe from Figure 5, that for $\mathcal{R}^d_{0C} < 1$, the number of infected individuals already introduced into the population declined rapidly to a disease free equilibrium point.

The observation from 8 establishes that fact that at $\mathcal{R}^d_{0C} < 1$, COVID-19 diseases becomes extinct as it approach a zero endemic point. Further, it is observed from Figure 8 that an increase in the transmission rates from $\beta_C = 0.3$ to $\beta_C = 0.6$ led to increases in the Reproductive number, which translates into increases in the number of infective population over time, as well as an increase in the time to endemic equilibrium. Numerical simulations of the model in Figure 8 also suggest that increasing compliance to protective measures κ or the decreasing disease transmission rates results in a reduction of $\mathcal{R}^d_{0C}$, thus, reduces the average number of COVID-19 infections in the population leading to extinction of the disease. We therefore suggest that all persons comply to preventive measures including social distancing, wearing facial mask, and the use of alcohol based sanitizer.

4.3 Co-infection Model

From the parameter values in Table 2, we calculated the reproductive number of co-infection model to be $\mathcal{R}^d_{0aC} = 2.3311$ for $(\beta_C = 0.5, \beta_a = 0.4)$. The result implies that on the average, an infected person introduced into the population can infect more than two susceptible, hence, the infection will continue. The trajectories of susceptible, infectious, treatment, recovered classes and other compartments in the co-infection model (3) are displayed in Figure 10. Here, we fixed values of all parameters shown in Table 2.

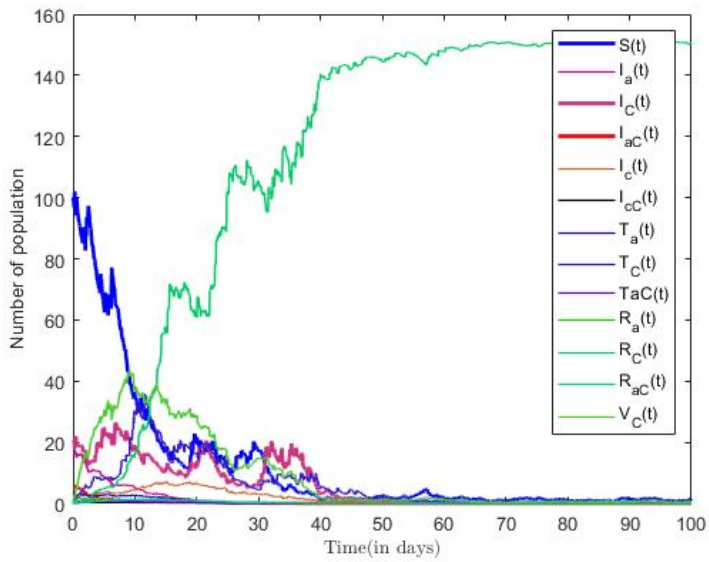

Figure 10: Solution for Co-infection Model $(\kappa = 0.5, \delta = 0.7, \zeta = 0.6)$.

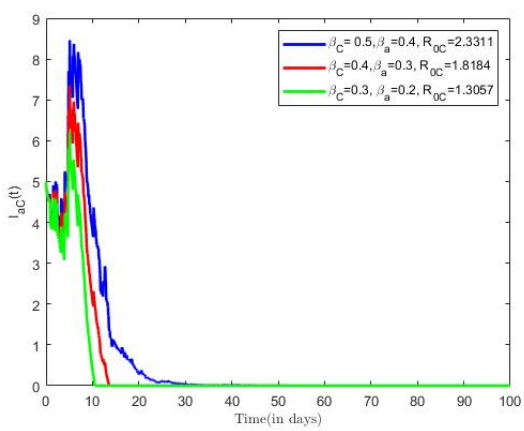

Figure 11: Co-Infection with varied effective contact rate and $\delta = 0.7, \kappa = 0.5, \zeta = 0.6$.

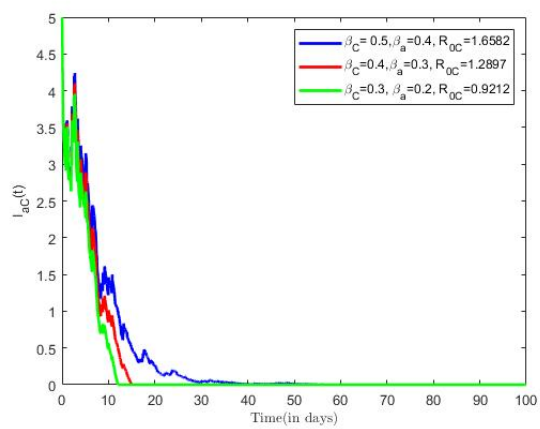

Figure 12: Co-infected population with varied transmission rate and $\delta = 0.9, \kappa = 0.9, \zeta = 0.6$.

From Figure 10, we observe that as number of co-infectious population increase in time, the susceptible population decrease. However, in the long run, the solution curves for both the susceptible and infective compartments behave like decreasing functions and approach a fixed point. A

decrease in the number of susceptible individuals occurred rapidly within the first fifteen time steps of the epidemic, after which there was gradual decline over time. We also increase in the number infected, Treatment and other compartments over the period. Eventually, infectious, recovered classes and other classes approach a fixed point in the long run. In other words, the results suggest that all compartments will reach their respective endemic fixed point of model (3) within a finite time and in long run. The numerical outcomes verifies that when $\mathcal{R}^s_{0aC} > 1$, then the disease endemic equilibrium is locally and globally asymptotically stable.

The impact of various parameters on the transmission dynamics of HBV is explored. Numerical results are presented in Figure 11 and Figure 12. We proceeded by first investigating the effects of transmission rate on population of infected individuals. This was done using varied pairs of values of transmission rates ($\beta_a = 0.2, 0.3, 0.4$), and ($\beta_C = 0.3, 0.4, 0.5$), while all remaining parameter values of the model were held constant. From Figure 11, we observe that as values of transmission rate increases, there is an increased possibility for the population to be co-infected with HBV, and COVID-19. Further, we investigated the effects of the transmission rate on the reproductive number of the co-infection model using the aforementioned rates . The estimated Reproductive numbers as 1.3057, 1.8184, and 2.3311 respectively. It is observed from Figure 11 that an increase in the transmission rates , β_a, and β_C, resulted in increases in the Reproductive number, which translates into increases in the number of infective population over time, as well as an increase in the time to endemic equilibrium.

Next, we investigated the effects of the compliance with preventive measures on the reproductive number of the Co-infection model. Here, we increased κ from 0.7 to 0.9, δ from 0.7 to 0.9, all other parameters were held constant, which earlier paired varied transmission rates ($\beta_a = 0.2, 0.3, 0.4$), and ($\beta_C = 0.3, 0.4, 0.5$) were utilised. We estimated Reproductive numbers as 0.9212, 1.2897 and 1.6582 respectively. It is observed from Figure 12 that an increase both COVID-19 and HBV compliance rate resulted in a reduction of the Reproductive number, which translates into decreases in the number of co-infective population over time as compared to Figure 11.

Numerical simulations of the model in Figure 12 also suggest that increasing compliance to COVID-19 and HBV preventive measures will results in a reduction of number of co-infected individuals in the population leading to extinction of the disease. We therefore suggest that all persons comply to preventive measures including social distancing, wearing facial mask, and the use of alcohol based sanitizer, HBV vaccination, safe sexual practices, desist from the sharing syringes, and ensuring healthcare providers use sterile.

5 Conclusion

The majority of issues in the real world are not deterministic. Because of its proximity to ambient sounds, the stochastic models allow us to model epidemic diseases in a more realistic manner.

In this paper, two distinct diseases were used to study a stochastically perturbed SITRVS-type model. An emphasis was placed on explaining the effect of small fluctuations and perturbations due to sudden environmental shocks in the transmission dynamics of the co-infection, hence the inclusion of Poisson-driven Lévy noise. To determine the conditions for the local asymptotic stability of the equilibria, we first computed the reproductive number and the equilibria for the underlying stochastic model (3). Furthermore, we investigated the conditions of extinction and persistence of HBV only, COVID-19 only, and co-infection models. We observe that persistence for all sub-models and co-infection model were dependent on the intensity of the Brownian noise and the values of epidemic parameters involved in disease transmission.

Additionally, we demonstrated the influence of different parameters on the infectious compartments by presenting several numerical simulation results using the Euler-Murayama scheme.

6 Declarations

6.1 Availability of data and materials

The authors confirm that the data used in this study are available within the article.

6.2 Competing Interest

The authors declare that they have no competing interests.

6.3 Funding

This research did not receive any funding.

6.4 Authors' Contribution Statement

MAP made the main contribution to this manuscript including theoretical formulation, analysis and simulations. **SEM** supplied several suggestions in theoretical part, editing and proofreading the manuscript. **SMN** supplied several suggestions in theoretical part, editing and proofreading the manuscript. All authors read and approved the final manuscript.

References

[1] Din A., Amine S., and Allali A. A stochastically perturbed co-infection epidemic model for covid-19 and hepatitis b virus. *Nonlinear Dynamics*, 111(2):1921–1945, (2023).

[2] Korobeinikov A. Lyapunov functions and global stability for sir and sirs epidemiological models with non-linear transmission. *Bulletin of Mathematical biology*, 68:615–626, 2006.

[3] Omame A., Mujahid M., Abbas, and Onyenegecha C. P. A fractional order model for the co-interaction of covid-19 and hepatitis b virus. *Results in Physics*, 37:105498, 2022.

[4] Pusparani A., Henrina J., and Cahyadi A. Co-infection of covid-19 and recurrent malaria. *The Journal of Infection in Developing Countries*, 15(05):625–629, (2021).

[5] Rehman A., Singh R., and Agarwal P. Modeling, analysis and prediction of new variants of covid-19 and dengue co-infection on complex network. *Chaos Solitons Fractals*, 150(111008):111008, 2021.

[6] Schweitzer A., Horn J., Mikolajczyk R. T., Krause G., and Ott J. J. Estimations of worldwide prevalence of chronic hepatitis b virus infection: a systematic review of data published between 1965 and 2013. *The Lancet*, 386(10003):1546–1555, 2015.

[7] Gumel A. B., Iboi E. A., Ngonghala C. N., and Ngwa G. A. Towards achieving a vaccine-derived herd immunity threshold for covid-19 in the u.s. *medRxiv*, 2021.

[8] Abioye A. I., Peter O. J., Ogunseye H. A., Oguntolu F. A., Ayoola T. A., and Oladapo A. O. A fractional-order mathematical model for malaria and COVID-19 co-infection dynamics. *Healthcare Analytics*, 4:100210, 2023.

[9] Tesfaye A. W. and Satana T. S. Stochastic model of the transmission dynamics of covid-19 pandemic. *Advances in Difference Equations*, 2021:1–21, (2021).

[10] Ji C., Jiang D., and Shi N. The behavior of an sir epidemic model with stochastic perturbation. *Stochastic Analysis and Applications*, 30(5):755–773, (2012).

[11] Center for Disease Control and Prevention. Sexually transmitted infections treatment guidelines, 2021: Hepatitis b virus (hbv) infection, 2021.

[12] Center for Disease Control and Prevention. Prevalence of the hepatitis b virus, 2024.

[13] CGHE. Ghana national hepatitis elimination profile: Key takeaways, January 2022.

[14] Otoo D., Donkoh E. K., and Kessie J. A. Estimating the basic reproductive number of covid-19 cases in ghana. *European Journal of Pure and Applied Mathematics*, 14(1):135–148, 2021.

[15] Iboi E. A., Ngonghala C. N., and Gumel A. B. Will an imperfect vaccine curtail the covid-19 pandemic in the us? *Infectious Disease Modelling*, 5:510–524, (2020).

[16] Agusto F. B., Numfor E., Srinivasan K., Iboi E. A., Fulk A., Saint O., Jarron M., and Peterson A. T. Impact of public sentiments on the transmission of covid-19 across a geographical gradient. *PeerJ*, 11:e14736, 2023.

[17] Agusto F. B., Erovenko I. V., Fulk A., Abu-Saymeh Q., Romero-Alvarez D., Ponce J., Sindi S., and J. M. Saint Onge O., Ortega, and Peterson A. T. To isolate or not to isolate: the impact of changing behavior on covid-19 transmission. *BMC Public Health*, 22(1):138, 2022.

[18] Friedman and Siewe N. Chronic hepatitis b virus and liver fibrosis: A mathematical model. *PLoS One*, 13(4):e0195037, 2018.

[19] Contreras G., Mora M. R., and Gómez P. J. Estimation of the epidemiological evolution through a modelling analysis of the covid-19 outbreak. *Microbiology*, 3:152–158, (2020).

[20] Tilahun G. T. and Alemneh H. T. Mathematical modeling and optimal control analysis of covid-19 in ethiopia. *Journal of Interdisciplinary Mathematics*, 24(8):2101–2120, 2021.

[21] Ghana Business News. Some 42 people die everyday in ghana from hepatitis b and c related diseases. *Ghana Business News*, September 2024. Accessed: 2025-05-10.

[22] Ghana Health Service. 2016 annual report. Technical report, Ghana Health Service, 2017.

[23] Branswell H. and Joseph A. Who declares the coronavirus outbreak a pandemic. *Stat*, 11, 2020.

[24] Rwezaura H., Diagne M. L., Omame A., de Espindola A. L., and Tchuenche J. M. Mathematical modeling and optimal control of sars-cov-2 and tuberculosis co-infection: a case study of indonesia. *Modeling Earth Systems and Environment*, 8:5493—5520, (2022).

[25] Adu I. K., Aidoo A. Y., Darko I. O., and Osei-Frimpong E. Mathematical model of hepatitis b in the bosomtwe district of ashanti region, ghana. *Applied Mathematical Sciences*, 8(67):3343–3358, 2014.

[26] Hezam I. M., Foul A., and Alrasheedi A. A dynamic optimal control model for COVID-19 and cholera co-infection in yemen. *Adv. Differ. Equ.*, 2021(1), December 2021.

[27] IndexMundi. Ghana - birth rate, n.d. Retrieved May 31, 2025.

[28] Kiyosi Itô and Takeyuki Hida, editors. *Stochastic Processes and Their Applications: Proceedings of the International Conference held in Nagoya, July 2-6, 1985*, volume 1203 of *Lecture Notes in Mathematics*. Springer-Verlag Berlin Heidelberg, Berlin, Heidelberg, 1986.

[29] Danane J., Allali K., and Hammouch Z. Mathematical analysis of a fractional differential model of hbv infection with antibody immune response. *Chaos, Solitons & Fractals*, 136:109787, 2020.

[30] Wang J. and Tian X. Global stability of a delay differential equation of hepatitis b virus infection with immune. *Electron. J. Differ. Equ.*, 94:1–11, (2013).

[31] Ott J. J., Stevens G. A., Groeger J., and Wiersma S. T. Global epidemiology of hepatitis b virus infection: new estimates of age-specific hbsag seroprevalence and endemicity. *Vaccine*, 30(12):2212–2219, 2012.

[32] Wu J. T., Leung K., and Leung G. M. Nowcasting and forecasting the potential domestic and international spread of the 2019-ncov outbreak originating in wuhan, china: a modelling study. *The Lancet*, 395(10225):689–697, (2020).

[33] Tobias Jahnke. Numerical methods in mathematical finance, 2016.

[34] Mekonen K. G. and Obsu L. L. Mathematical modeling and analysis for the co-infection of COVID-19 and tuberculosis. *Heliyon*, 8(10):e11195, October 2022.

[35] Böttcher L. and Nagler J. Decisive conditions for strategic vaccination against sars-cov-2. *Chaos*, 31(10):101105, 2021.

[36] Wee L. E., J. Y. Tan, Oon L. L. E., Pena A. M. T., Quek J. K. S., Venkatachalam I., Ko K. K., and Wijaya L. Relapsing COVID-19 infection as a manifestation of good syndrome: a case report and literature review. *Int. J. Infect. Dis.*, 129:236–239, apr 2023.

[37] Allen L. J. *An introduction to stochastic processes with applications to biology*. CRC press, 2010.

[38] El Fatini M., El Khalifi M., Gerlach R., Laaribi A., and Taki R. Stationary distribution and threshold dynamics of a stochastic sirs model with a general incidence. *Physica A-statistical Mechanics and Its Applications*, 534:120696, (2019).

[39] Ray M., Vazifdar A., and Shivaprakash S. Co-infection with malaria and coronavirus disease-2019. *Journal of Global Infectious Diseases*, 12(3), (2020).

[40] Ashinyo M. E., Duti V., Dubik S. D., Amegah K. E., Kutsoati S., Oduro-Mensah E., Puplampu P., Gyansa-Lutterodt M., Darko D. M., Buabeng K. O., A. Ashinyo, A. A. Ofosu, Baddoo N. A., Akoriyea S. K., Ofei F., and Kuma-Aboagye P. Clinical characteristics, treatment regimen and duration of hospitalization among covid-19 patients in ghana: a retrospective cohort study. *Pan African Medical Journal*, 37:9, 2020.

[41] Hama M. F., Rasul R. R. Q., Hammouch Z., Rasul K. A. H., and Danane J. Analysis of a stochastic seis epidemic model with the standard brownian motion and lévy jump. *Results in Physics*, 37:105477, (2022).

[42] Diagne M. L., Rwezaura H., Tchoumi S. Y., and Tchuenche J. M. A mathematical model of covid-19 with vaccination and treatment. *Computational and Mathematical Methods in Medicine*, 2021:1250129, (2021).

[43] Ojo M. M. and Goufo D. F. E. The impact of covid-19 on a malaria dominated region: A mathematical analysis and simulations. *Alexandria Engineering Journal*, 65:23–39, (2023).

[44] Johns Hopkins University & Medicine. Coronavirus resource center, 2020. Accessed: 2024-12-13.

[45] Dalal N., Greenhalgh D., and Mao X. A stochastic model of aids and condom use. *Journal of Mathematical Analysis and Applications*, 325(1):36–53, 2007.

[46] C. Okeahalam, V. Williams, and K. Otwombe. Factors associated with covid-19 infections and mortality in africa: a cross-sectional study using publicly available data. *BMJ Open*, 10:e042750, 2020.

[47] Graphic Online. Health minister confirms 107 covid-19 cases at university of ghana, July 2025. Accessed 23 July 2025.

[48] World Health Organization. COVID-19 vaccination in humanitarian settings. `https://www.who.int/publications/i/item/9789240079434`, (2023). [Online; accessed 25 October 2023].

[49] Boonyarangka P., Phontham K., Sriwichai S., Poramathikul K., Harncharoenkul K., Kuntawunginn W., Maneesrikhum N., Srisawath S., Seenuan C., Thanyakait C., Inkabajan K., Pludpiem S., Pidtana K., Demons S., Vesely B., Wojnarski M., Griesenbeck J. S., and Spring M. Co-infection with plasmodium vivax and covid-19 in thailand. *Tropical Medicine and Infectious Disease*, 7(8), (2022).

[50] Das P., Upadhyay R. K., Misra A. K., Rihan F. A., Das P., and Ghosh D. Mathematical model of covid-19 with comorbidity and controlling using non-pharmaceutical interventions and vaccination. *Nonlinear Dyn.*, 106:1213–1227, (2021).

[51] M. A. Pobbi, S. M. Naandam, and S. E. Moore. Mathematical modelling and analysis of stochastic malaria and covid-19 co-infection model. *Applied Mathematics in Science and Engineering*, 33(1), 2025.

[52] Zhao S., Xu Z., and Lu Y. A mathematical model of hepatitis b virus transmission and its application for vaccination strategy in china. *International journal of epidemiology*, 29(4):744–752, 2000.

[53] Manu S. D. Ghana covid-19 dataset. "https://www.kaggle.com/ds/657993", 2020.

[54] Moore S. E., Nyandjo-Bamen H. L., Menoukeu-Pamen O., Asamoah J. K. K., and Jin Z. Global stability dynamics and sensitivity assessment of covid-19 with timely-delayed diagnosis in ghana. *Computational and Mathematical Biophysics*, 10(1):87–104, 2022.

[55] Shah S. M. A., Nie Y., Din A., and Alkhazzan A. Dynamics of hepatitis b virus transmission with a lévy process and vaccination effects. *Electron. J. Differ. Equ.*, 12:16–45, (2024).

[56] Teklu S. W. Analysis of hbv and covid-19 coinfection model with intervention strategies. *Comput Math Methods Med.*, (2023).

[57] Tchoumi S. Y., Diagne M. L., Rwezaura H., and Tchuenche J. M. Malaria and covid-19 co-dynamics: A mathematical model and optimal control. *Applied mathematical modelling*, 99:294–327, (2021).

[58] Sun T., Chi H., Wang J., Zheng Y., Zhu H., Zhao J., Zhou K., Chen M., and T. Tung D., Wang, et al. Effect of sars-cov-2 infection on liver function in patients with hepatitis b. *BMC Infectious Diseases*, 24:1428, 2024.

[59] Solomon Weldegebriel Teklu. Impacts of optimal control strategies on the hbv and covid-19 co-epidemic spreading dynamics. *Scientific Reports*, 14(1):5328, 2024.

[60] Botwe W. K. Deterministic sir model of hepatitis b virus infection and the impact of vaccination (the case of sunyani municipality), 2023.

[61] World Health Organization. Hepatitis b: Key facts and prevalence in africa. Accessed: 2025-01-12.

[62] World Health Organization. Hepatitis b. "https://www.who.int/news-room/fact-sheets/detail/hepatitis-b", April 9 2024. Accessed: 2025-01-12.

[63] Chen X., Jiang Q., Ma Z., Ling J., Hu W., Cao Q., Mo P., Yao L., Yang R., Gao S., Gui X., Hou W., Xiong Y., Li J., and Zhang Y. Clinical characteristics of hospitalized patients with sars-cov-2 and hepatitis b virus co-infection. *Virol Sin.*, 35:842–845, (2020).

[64] Wang X., Wang C., and Wang K. Extinction and persistence of a stochastic sica epidemic model with standard incidence rate. *Advances in Difference Equations*, (2021).

[65] Maria Xiridou, Philippe Adam, Annemarie Meiberg, Maartje Visser, Amy Matser, John De Wit, and Eline Op De Coul. The impact of the covid-19 pandemic on hepatitis b virus vaccination and transmission among men who have sex with men: A mathematical modelling study. *Vaccine*, 40(33):4889–4896, 2022.

[66] Lin Y., Yuan J., Long Q., Hu J., Deng H., Zhao Z., Chen J., Lu M., and Huang A. Patients with sars-cov-2 and hbv co-infection are at risk of greater liver injury. *Genes & Diseases*, 8(4):484–492, 2021.

[67] Sabbar Y. *Mathematical Analysis of Some Stochastic Infectious Disease Models with White Noises and Lévy Jumps*. PhD thesis, Université Sidi Mohamed Ben Abdellah de Fès (Maroc), (2021).

[68] Nartey Y. A., Okine R., A. Seake-Kwawu, G. Ghartey, Y. K. Asamoah, K. Senya, A. Duah, A. Owusu-Ofori, J. Amugsi, D. Suglo, S. A. Bampoh, L. Hiebert, H. Njuguna, J. W. Ward, A. Plymoth, L. R. Roberts, A. S. Bockarie, Y. A. Awuku, and Obiri-Yeboah D. A nationwide cross-sectional review of in-hospital hepatitis b virus testing and disease burden estimation in ghana, 2016 - 2021. *BMC Public Health*, 22:2149, 2022.

[69] Zhang Z., Zeb A., Hussain. S., and Alzahrani E. Dynamics of COVID-19 mathematical model with stochastic perturbation. *Advances in Difference Equations*, 2020(1):451, (2020).